A Chiral Vanadium(V) Complex-catalyzed Enantioselective Oxidative Homo- and Hetero-coupling of Hydroxycarbazoles

大阪大学

Osaka University

A Ph.D. Thesis

Submitted to the Department of Chemistry

Graduate School of Science

Osaka University

By

Ganesh Tatya Kamble

Department of Synthetic Organic Chemistry

August 2022

Ph.D. Thesis Title

A Chiral Vanadium(V) Complex-catalyzed

Enantioselective Oxidative Homo- and Hetero-coupling of Hydroxycarbazoles

ABSTRACT

Hydroxycarbazoles are one of the most important classes of molecules due to their biological activity from medicinal point of view. The carbazole framework is found in a wide range of bioactive natural products and pharmaceuticals, showing anti-viral, anti-malarial, and anti-tumour activity. Some of them are currently being used as lead compounds for drug development. The carbazoles are also used as building blocks for synthesising functional materials, such as organic light-emitting diodes (OLED), because of their wide band gap, high luminescence efficiency, and flexible modification of the parent skeleton.

Considering the importance of a variety of hydroxycarbazoles, I herein report the oxidative coupling reaction of hydroxycarbazoles to generate axially chiral bi-hydroxycarbazoles using a chiral vanadium complex. To fill the gap in research and deliver the straightforward synthetic method with high enantioselectivity; a detailed study on homo-coupling of 4-hydroxycarbazoles using dinuclear vanadium catalyst *via* a dual activation method is discussed in **Chapter 2.**

Among the synthesis of a hetero biaryl moiety, the challenge of hetero-coupling of hydroxycarbazoles with 2-naphthols (or β-ketoesters) has been successfully developed by utilizing mono nuclear vanadium complex in **Chapters 3 and 4.**

DECLARATION

The scientific study detailed in this thesis was completed for a Doctor of Philosophy degree in Synthetic Organic Chemistry at Osaka University's Graduate School of Science, Department of Chemistry, between October 2019 and September 2022. It is the Author's work unless otherwise noted, and it has not been presented in whole or in part to support an application for another degree or qualification at this or any other university or institute of learning.

Ganesh Tatya Kamble

Signed: _____ Date: 2022/08/30

List of Symbols and Abbreviations

Ac	acetyl
APCI	atmospheric pressure chemical ionization
aq.	aqueous solution
Ar	aryl
BINAP	2,2'-bis(diphenylphosphino)-1,1'-binaphthyl
BINOL	1,1'-bi-2-naphthol
Bn	benzyl
cat.	catalyst
CD	circular dichroism
Cp	cyclopentadienyl
CPL	circularly polarized luminescence
Cod	1,5-cyclooctadiene
Conv.	conversion
dba	tris(dibenzylideneacetone)dipalladium(0)
DCB	1,2-dichlorobenzene
DCE	1,2-dichloroethane
DCM	dichloromethane
DDQ	2,3-dichloro-5,6-dicyano-*p*-benzoquinon
DMF	*N*,*N*-dimethylformamide
Ee	enantiomeric excess
Eq	equation
Equiv	equivalent
ESI	electrospray ionization
Et	ethyl
GPC	gel permeation chromatography
HPLC	high performance liquid chromatography
HRMS	high resolution mass spectrometry
HFIP	hexafluoro isopropyl alcohol
***i*-Pr**	isopropyl
IR	infrared
L	ligand
Me	methyl

MOP	2-diphenylphosphino-2'-methoxy-1,1'-binaphthyl
MS	mass
MS 3A, 4A or 5A	molecular sieves 3A, 4A or 5A
MW	microwave
***n*-Bu**	*normal*-butyl
NMR	nuclear magnetic resonance
PIFA	(bis(trifluoroacetoxy)iodo) benzene
Ph	phenyl
PL	photoluminescence
Quant	quantitative
Rac	racemic
Rt	room temperature
Segphos	5,5’-bis(diphenylphosphino)-4,4’-bi-1,3-benzodioxole
***t*-Bu**	*tert*-butyl
TBME	*tert*-butyl methyl ether
TBAF	tetrabutylammonium fluoride
Tf	trifluoromethyl
THF	tetrahydrofuran
TMEDA	*N*, *N*, *N*, *N*-tetramethyl ethylenediamine
TMS	trimethylsilyl
Ts	*p*-toluene sulfonyl
UV	ultraviolet
***p*-TSA**	*p*-toluene sulfonic acid
[Φ]	molar optical rotation
TLC	thin layer chromatography
ORTEP	Oak Ridge thermal ellipsoid plot
Ppm	part(s) per million

TABLE OF CONTENTS

Chapter 1: Introduction

The structural motifs containing chiral biaryls have been extensively studied over the decades due to their potential applications in asymmetric synthesis.[1] A noteworthy contribution was therefore made by organic chemists to develop various biaryls using novel synthetic strategies. Especially, 6,6′-dinitrobiphenyl-2,2′-dicarboxylic acid and relative molecules are interesting moieties as they were found to have an axial chirality seen in structures made up of crossing dissymmetric planes.[2] In fact, the atropisomers of chiral biaryls are encountered in various synthetic compounds such as chiral ligands and catalysts as well.[3-5] The presence of chiral biaryls is not limited only to the chiral ligands and catalysts but is also seen in the natural products of pharmaceutical interest as shown in the (**Figure 1**).[6]

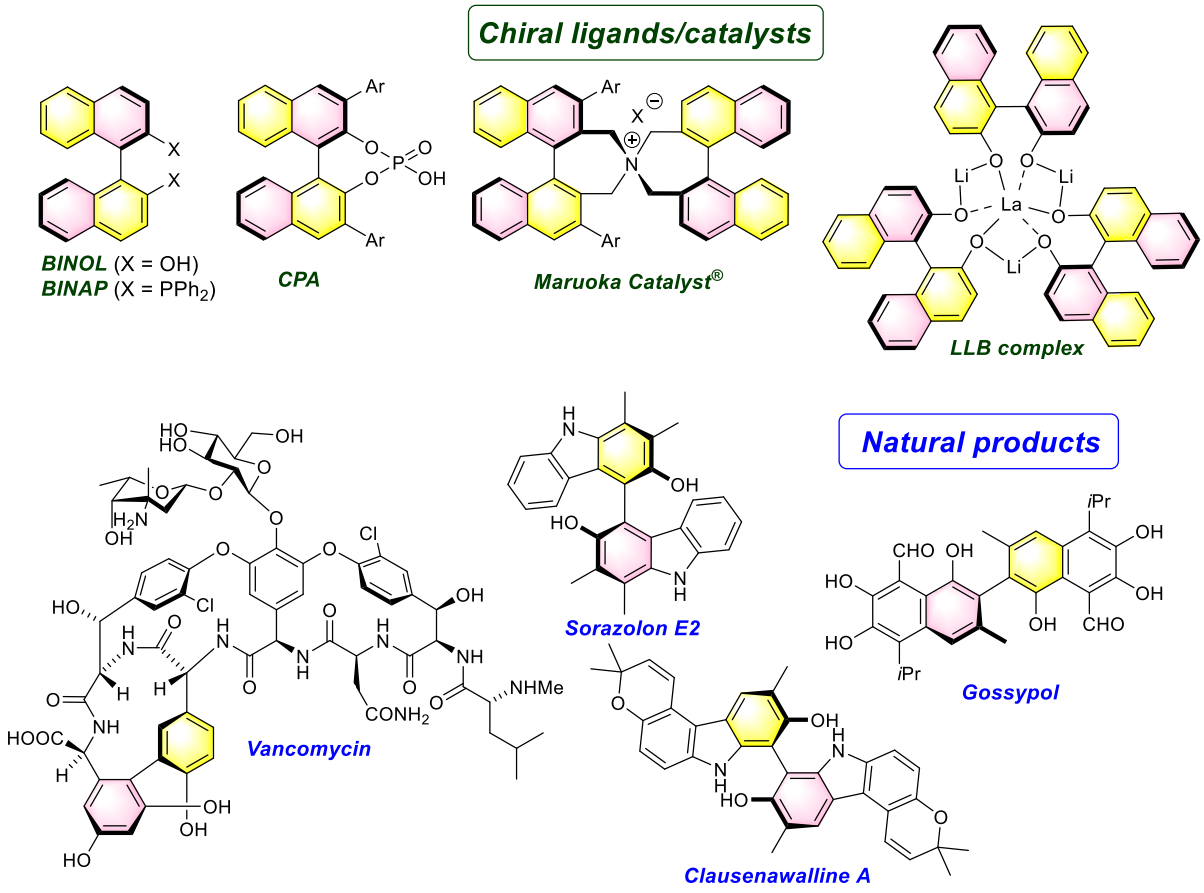

Figure 1. Representative examples of axially chiral ligands, catalysts, and natural products

A notable contribution toward the synthesis of optically active biaryl derivatives is well reported in the literature. For instance, (A) an enantioselective coupling of aryls,[2a-c] (B) a chirality transfer from central chirality to axial chirality,[2d-e] and (C) kinetic resolution of racemic compounds or atroposelective transformation of prochiral compounds[2f-g] are some of

the representative examples as shown in the (**Scheme 1**). Additionally, (D) the transition-metal-catalyzed benzannulations such as [2+2+2] annulations also allowed the generation of chiral biaryls; which is an excellent alternative construction of axial chirality.[2h]

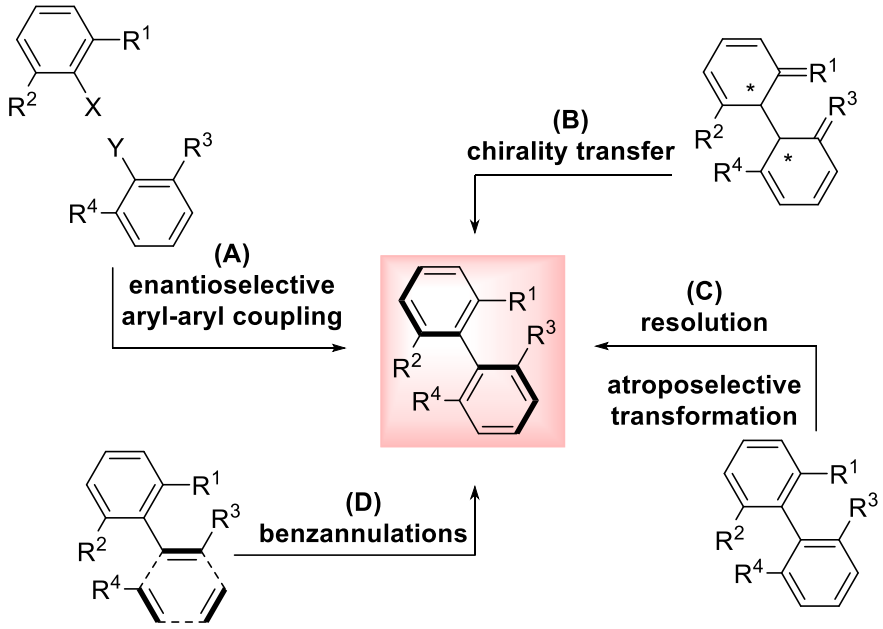

Scheme 1. Representative strategies for optically active biaryl derivatives

The catalytic synthesis of biaryls is challenging due to low yield, low stereochemical control, and side product formations. In this context, several research groups have developed facile strategies for the synthesis of functionalized biaryls. Among them, the metal complex-catalyzed enantioselective construction of axially chiral scaffolds has been widely explored. Especially, chiral base metal complex-catalyzed oxidative homo- and hetero-coupling of arenol derivatives is one of the most straightforward and sustainable approaches. Indeed, this strategy is advantageous from the synthesis point of view as it does not require any pre-activation for the coupling partners. Consequently, highly active chiral catalysts for the oxidative coupling of arenols [2a, c,7] have been reported during the last few years.

However, the number of methods for the enantioselective synthesis of axially chiral biarenols such as phenols, polycyclic and heterocyclic arenols are still limited due to high oxidation potentials require strong oxidants (or low oxidation potentials needing adequate conditions) to suppress over-oxidations. Especially, when compared to that the catalytic and highly enantioselective synthesis of 1,1′-bi-2-naphthol (BINOL) derivatives using chiral metal catalysts. Some of the examples are outlined in (**Figure 2**) containing [mononuclear metal catalysts: Smrcina and Kocovsky (Cu 1993),[8a] Nakajima (Cu 1999),[8b] Katsuki (Ru 2000),[8c]

Kozlowski (Cu 2001),[8d] Chen (V 2002),[8e] Uang (V 2003),[8f] Iwasawa (V 2004),[8g] Ha (Cu 2004),[8h] Habaue (V, Cu 2005),[8i-j] Sekar (Cu 2013),[8k] Cui and Wu (Cu 2014),[8l] Breuning (Cu 2015),[8m] Bania (V 2015),[8n] Pappo (Fe 2016, 2019),[8o-p] Sasai and Takizawa (V 2016),[9] Oh and Takizawa (V 2017),[9] Ishihara (Fe 2019)[8q] Tu and Tian (Cu 2019, 2021),[8r-s] Uchida (Ru 2020),[8t] and Zhang (Cu 2022)[8u] and dinuclear metal complexes: Gong (V 2002),[8v] Gao (Cu 2003),[8w] Sasai and Takizawa (V 2004),[10] Katsuki (Fe 2009)[8x]].

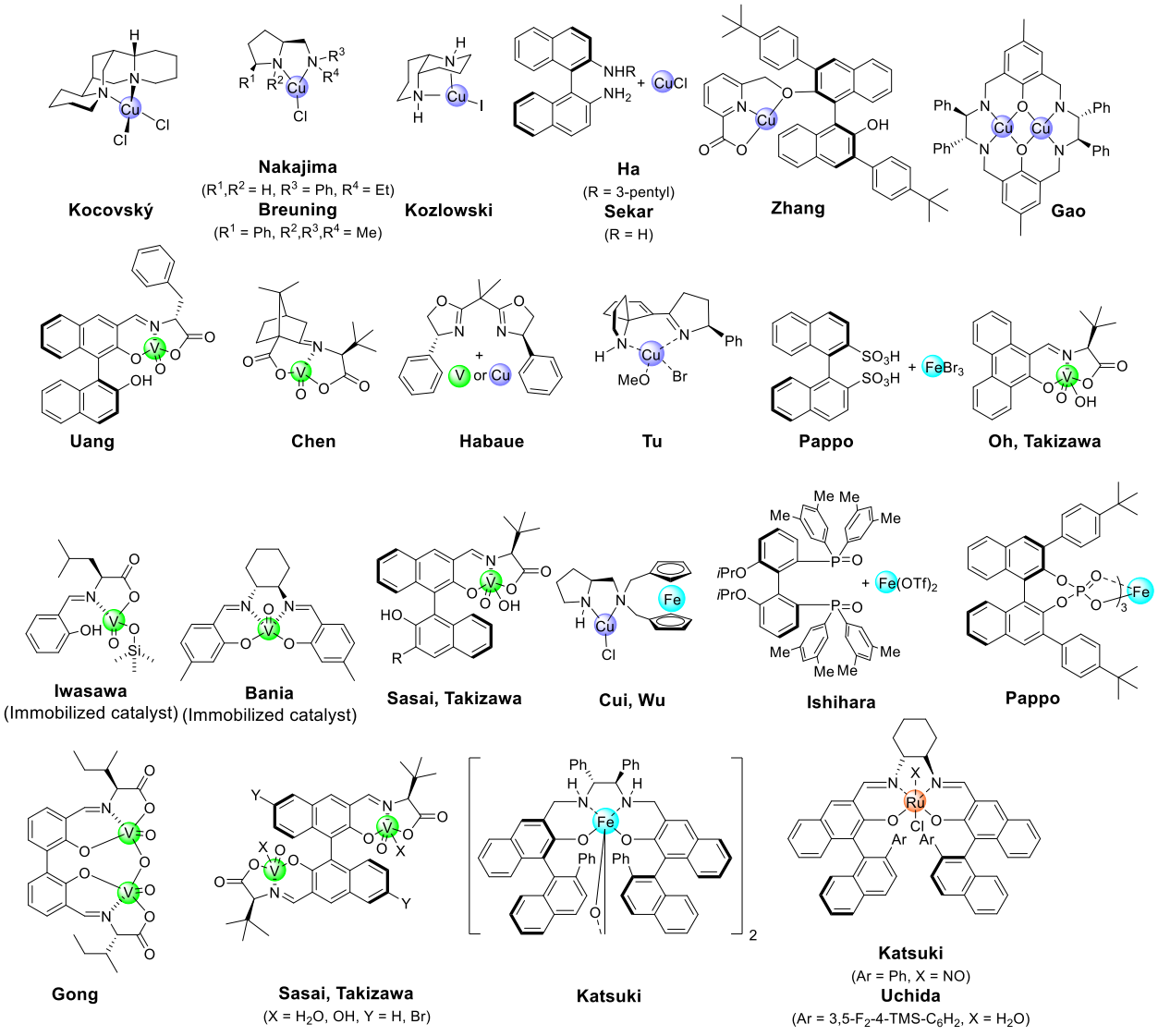

Figure 2. Highly active chiral transition metal catalysts for oxidative homo- and hetero-coupling of 2-naphthols

1.1 Reported Oxidative Coupling of Phenols and their Problems to be Solved

A hetero-coupling reaction involves binding two different reaction substrates to each other. The fabrication of the highly optically active and regioselective hetero-coupling is challenging even though using 2-naphthol coupling precursors. In most cases, the use of a high stoichiometric fraction of the substrate is essential due to the low gap between the oxidation potential and its effects on reactivity. In this context, the representative reports on hetero-coupling reactions using 2-naphthol analogues are shown in **Scheme 2-1.**

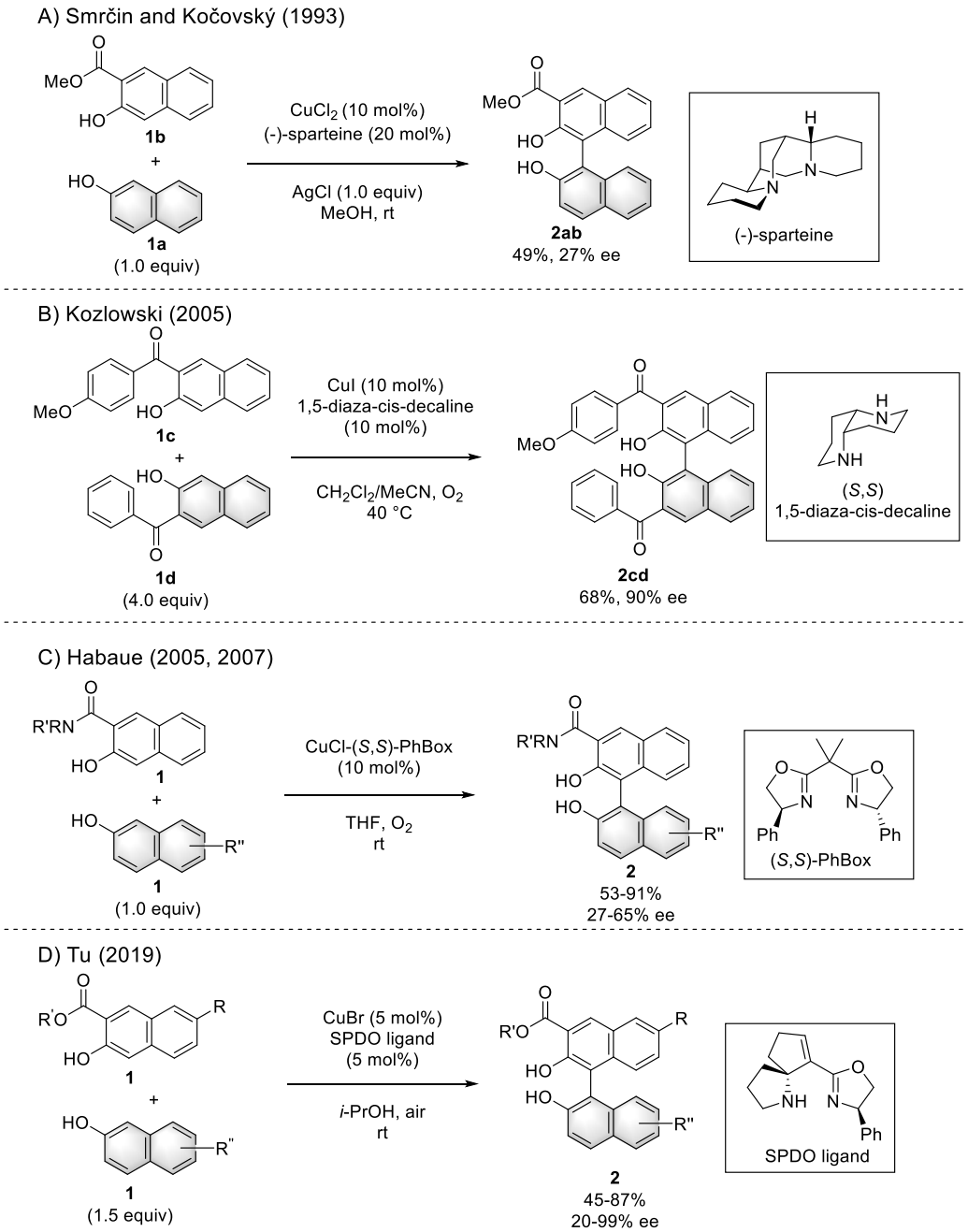

Scheme 2-1. The reported oxidative hetero-coupling of naphthol derivatives

In 1993, Smrčin and Kočovský *et al.* reported the synthesis of binaphthyl moiety **2ab** using a chiral copper catalyst prepared from copper (II) chloride and (-)-sparteine promoted oxidative hetero-coupling reaction using silver (I) chloride as an oxidant.[8a] Despite it being an interesting example of the chiral biaryls, the yield as well as enantioselectivity was not considerably promising. Later, Kozlowski *et al.* developed a copper (I) complex with 1,5-diaza-*cis*-decalin chiral ligand; which delivered an improved yield and enantioselectivity (90% ee) when using a 2-naphthol substrate with a carbonyl group at the C-3 position (**Scheme 2-1-B**);[22] molecular oxygen is adopted as an oxidizing agent.

In 2005 and 2007, Habaue *et al.* reported hetero-coupling reactions utilizing cuprous chloride and chiral oxazoline (*S, S*)-PhBoX ligands. **(Scheme 2-1-C)**.[23] When the reaction substrates were taken a stoichiometrically a 1:1 ratio product **2** was obtained with up to 91% yield and 65% ee along with high chemoselectivity. Most recently, Tu *et al.* reported a highly enantioselective hetero-coupling reaction using copper (I) bromide and a spiro skeleton SPDO ligand affording binaphthyl product **2** with up to 87% yield and 99% ee (**Scheme 2-1-D**).[24] This reaction also adopts molecular oxygen from the air, which is a co -oxidant.

Alternatively, the cheaper and safer Fe-metal catalysis was explored by Katsuki *et al.* for oxidative hetero-coupling reactions of 2-naphthols using Fe-Salen catalysts (**Scheme 2-2-A**).[25] This strategy affords chiral binaphthyl derivatives in moderate yields with excellent enantioselectivity.

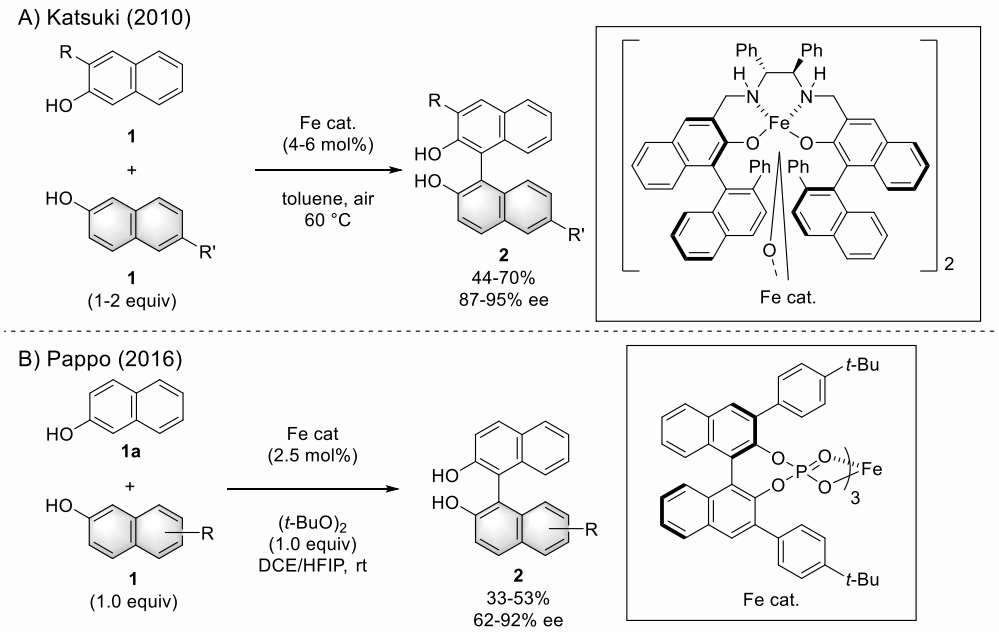

Scheme 2-2. The reported oxidative hetero-coupling of naphthol derivatives using Fe metal

Pappo *et al.* reported the utilization of chiral iron-phosphate complex for hetero-coupling using HFIP as a solvent to produce biaryl product **2** with up to 53% yield with 92% ee (**Scheme 2-2-B**).[8o] This methodology was valuable to deliver products with high enantioselectivity even when unsubstituted 2-naphthol substrates were used.

Apart from Fe and Cu catalysts, the electron-rich ruthenium complexes were also successfully explored for the synthesis of functionalized biaryls. Recently, Uchida *et al.* reported Ru-Salen catalysed hetero-coupling reaction to synthesize product **2** with up to 85% yield and 89% ee (**Scheme 2-3-A**).[8t] Interestingly, the unwanted homo-coupling reaction can be suppressed by the inclusion of bulky substituents at the C-3 and C-7 positions of the substrate. The catalyst is also suitable for oxidative hetero-coupling reactions between 2-naphthols and phenols, leading to product **2** with up to 67% yield and 90% ee.

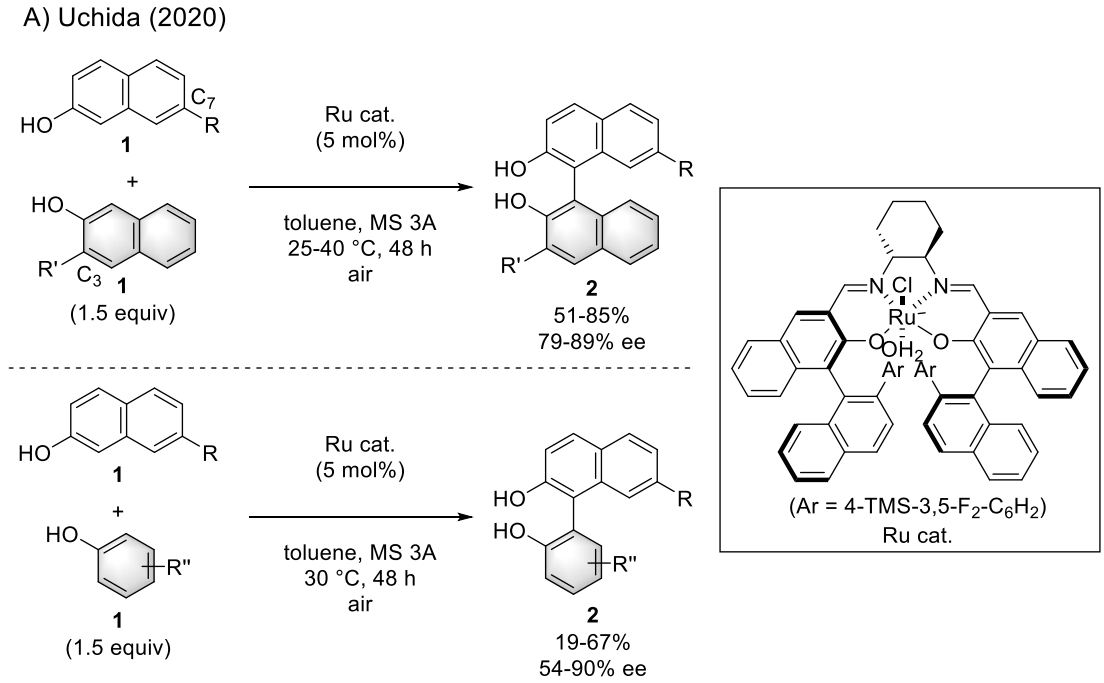

Scheme 2-3 The reported oxidative hetero-coupling of naphthol using Ru metal

It would be worth mentioning that the chemoselective synthesis of chiral C_1-symmetric bis(arenols) through enantioselective oxidative coupling with electronically comparable arenols without a directing group remains a challenge. Kozlowski and Pappo independently illustrated that the steric and/or electronic factors of the coupling partner such as the intensity of the binding to the metal catalyst, oxidation potential, and nucleophilicity are crucial considerations of cross-selective coupling.

The excessive exploitation of the substrates is also required to obtain the hetero-coupling products in high yields with high enantioselectivity. In addition, when a copper catalyst is used, a carbonyl group which is an oriented group at the C-3 perspective of the 2-naphthol substrate; a high substituent is anticipated for the reaction substrate. The chemical selectivity of the oxidative hetero-coupling is complicated, and it is vital to suppress the formation of homo-coupling and side reactions.

1.2 Dimeric Hydroxycarbazole in Natural Products

Carbazoles are tricyclic heterocycles made up of two six-membered benzene rings fused on either side of a five-membered nitrogen-containing ring of pyrrole. Functionalized carbazoles are one of the important classes of organic scaffolds which are present in many natural products.[11] Among them, the dimeric hydroxycarbazole derivatives have attracted many research groups due to their natural abundance and a broad spectrum of pharmacological actions such as anti-tumour, anti-oxidant, anti-bacterial activities, and free-radical scavenging effects. Moreover, the dimeric hydroxycarbazoles have also attracted attention as usage for C_2-symmetric chiral ligands. (**Figure. 3**)[12,13] However, only a few reports deal with enantioselective processes because their high reactivity leads to over-oxidation reactions.[14] Precise and gentle manufacturing processes for this important class of optically active compounds are still in great demand.

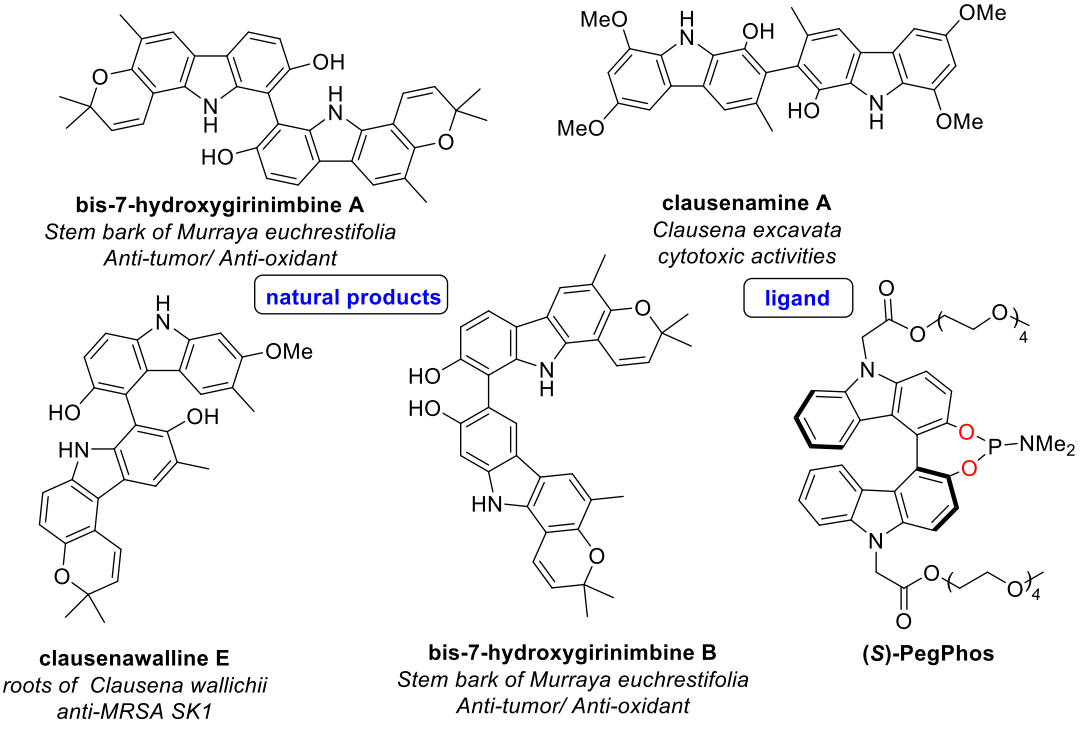

Figure 3. Dimeric hydroxycarbazoles in natural products and chiral ligands

1.3 Reported Homo-coupling of Hydroxycarbazole

Over the past decades, several synthetic strategies have been developed to obtain easy access to natural dimeric hydroxycarbazole derivatives. Especially, oxidative coupling of hydroxycarbazoles is one of the interesting methods of accessing these axially chiral molecules.[14] In 1989, the Moody research group reported the homo-coupling of 3-hydroxycarbazole in the presence of benzoyl peroxide along with manganese (VI) oxide as co-oxidant to synthesize the homo-coupled but optically inactive product as shown in the (**Scheme 3-A**).[15]

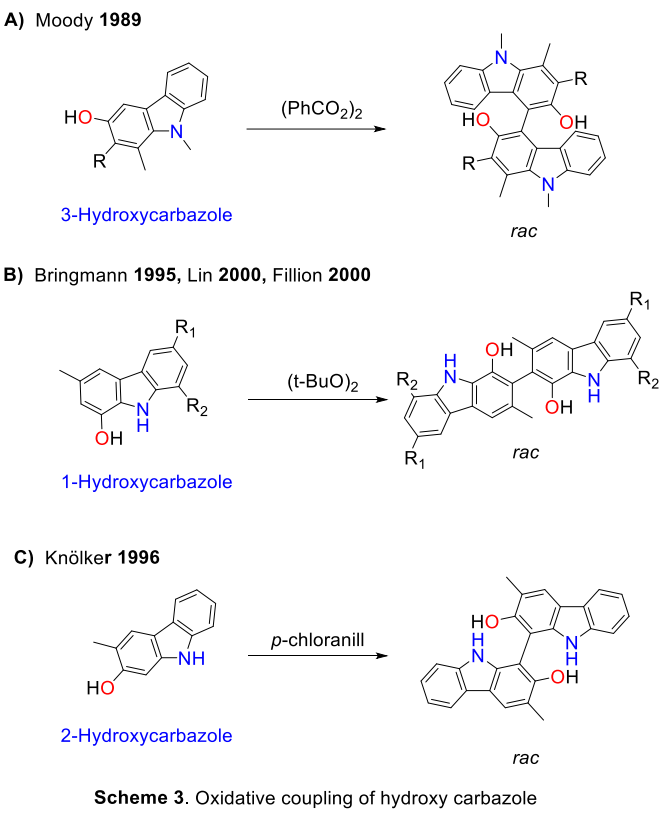

Scheme 3. Oxidative coupling of hydroxy carbazole

Bringmann, Lin, and Fillion independently reported the oxidative homo-coupling of 1-hydroxycarbazoles in the presence of *tert*-butyl peroxide as an oxidant as shown in (**Scheme 3-B**).[16] One year later from Bringmann, Knölker found that tetrachloro-para-benzoquinone worked as oxidative coupling reagents for 2-hydroxycarbazole (**Scheme 3-C**).[17] Moody and Knölker have adopted highly toxic reagents such as $Hg(OAc)_2$, $(FeCO)_5$, and $TI(TFA)_3$ respectively to synthesize hydroxycarbazole precursors for oxidative coupling. Before 2016, there was no substantial success in developing a green and enantioenriched oxidative coupling for hydroxycarbazoles.

Several attempts were made to establish an asymmetric evolution of axially chiral oxidative homo-coupling of hydroxycarbazoles**.** In 2015, the Kozlowski group reported the oxidative coupling of 2-hydroxycarbazole **3a** using a chiral vanadium catalyst **4a**. However, this methodology delivered products with poor enantio- and regioselectivities. Vanadium catalyst **4a** can activate both the ortho (C_1) and ortho' (C_3) positions near the hydroxyl group, leading to a formation of regio-isomeric oligomers (**Scheme 4-1**);[18] the chiral vanadium catalyst leading to the racemic product **6a** up to 70% yield as a Major product.

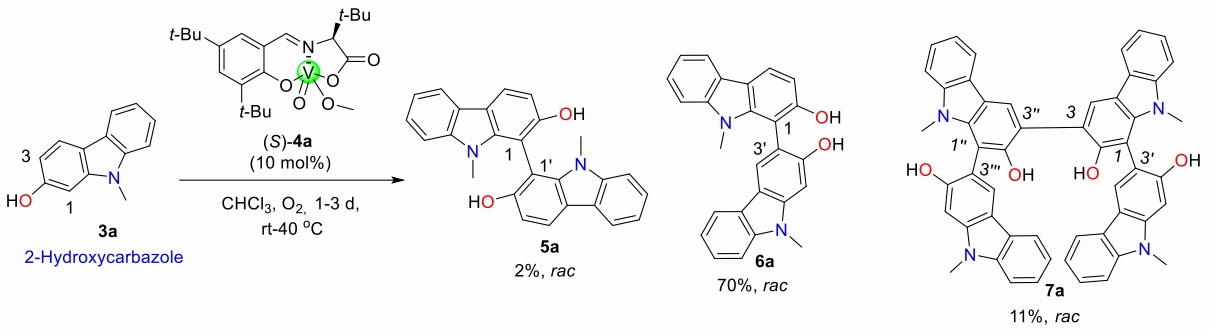

Scheme 4-1. First vanadium-catalyzed oxidative coupling of 2-hydroxycarbazoles

To suppress the formation of regioisomeric oligomers as well as racemized products, Kozlowski introduced a methyl group at the ortho'-carbon and benzyl substitution at the nitrogen atom of the 2-hydroxycarbazoles. Interestingly, the oxidative coupling of 2-hydroxycarbazole **3b** proceeds with an excellent yield and stereochemical control using chiral vanadium catalyst **4b**. The catalyst loading of 20 mol% successfully delivered the product **5b** with 91 % yield, and 87% ee (**Scheme 4-2**).[18b]

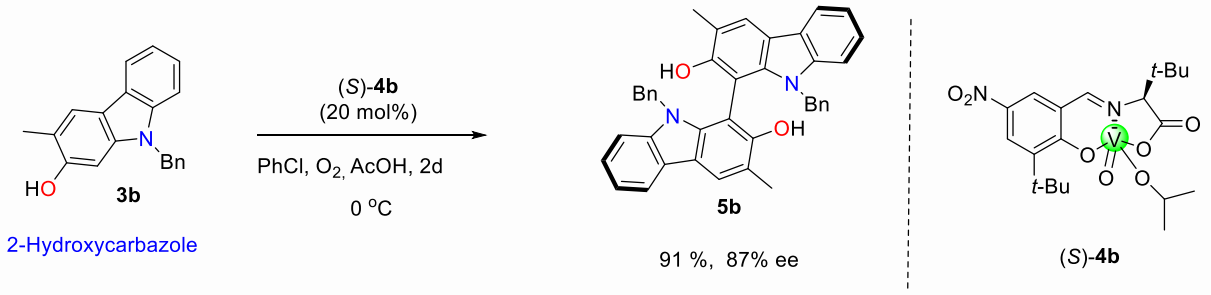

Scheme 4-2. Vanadium-catalyzed oxidative coupling of 2-hydroxycarbazoles

Recently, our group also reported the enantioselective oxidative coupling of 2-hydroxy-3-methylcarbazole using a chiral vanadium complex (R_a,*S*)-**8a** (**Scheme 4-3**).[19] The enantioselectivity of the product was observed low due to the racemization of the product in the absence of the *N*-protecting group.

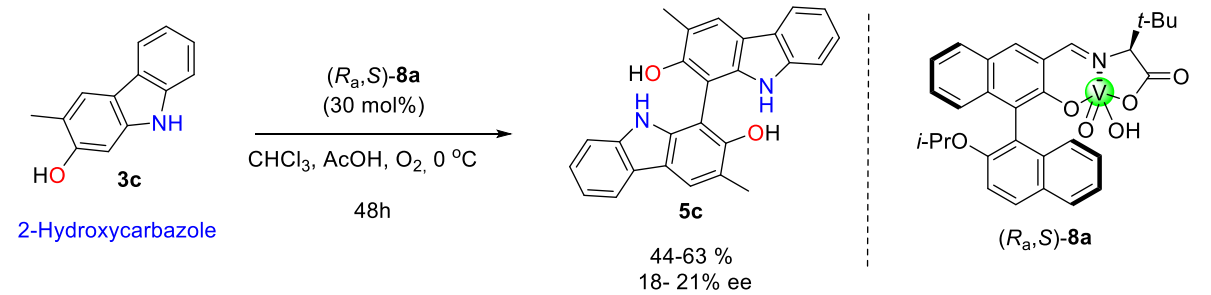

Scheme 4-3. Vanadium-catalyzed oxidative coupling of 2-hydroxycarbazoles

Subsequently, our group reported the first oxidative homo-coupling of 3- hydroxycarbazoles using dinuclear vanadium complex (R_a,*S*,*S*)-**10a** in the presence of air which serves as a co-

oxidant (**Scheme 5-1**).[19] It was observed that *N*-Phenyl-, 4-Cl-C_6H_4-, as well as 4-Me-C_6H_4-substituted substrates **9** afforded their corresponding homocoupling products **11** in moderate yields (55- 65%) with good enantioselectivities (75- 80% ee).

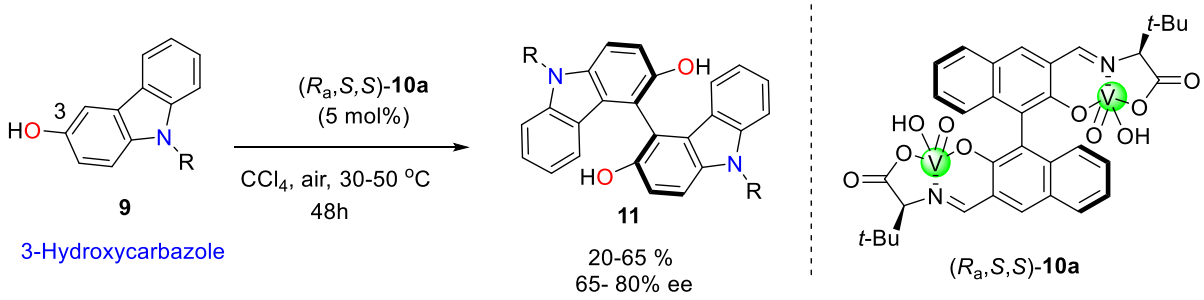

Scheme 5-1. Dinuclear Vanadium-catalyzed oxidative coupling of 3-Hydroxycarbazoles

Despite these successful reports on enantioselective oxidative coupling of 2- and 3-hydroxycarbazoles, there are still challenges with other relatively complex hydroxycarbazole derivatives. Consequently, it creates an opportunity to develop new strategies to synthesize homo-and hetero-coupled hydroxycarbazoles with high enantioselectivity and yields. The primary aim of my PhD thesis was to explore dinuclear and mononuclear vanadium complexes for the enantioselective synthesis of functionalized hydroxycarbazoles.

1.4 My work: homo- and hetero-coupling of hydroxycarbazoles

My research work was exclusively based on the enantioselective homo- and hetero-coupling of hydroxycarbazoles. The brief outline of my work is depicted as follows.

(i) Enantioselective oxidative couplings of 4-hydroxycarbazoles using a chiral dinuclear vanadium(V) complex (R_a,*S*,*S*)-**10a** have been achieved for the first time. The desired dimeric 4-hydroxycarbazole products were obtained with up to 90% ee under mild reaction conditions. Subsequently, the high racemization barriers of coupling products calculated by DFT indicated the potential usefulness of biaryl skeletons as C_2-symmetric chiral ligands for asymmetric catalysis.[20]

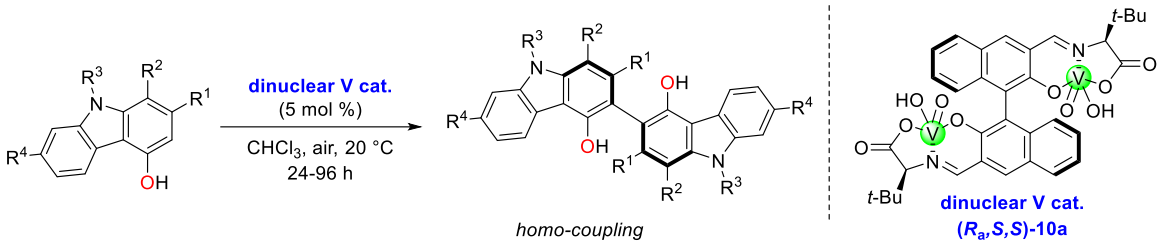

The detailed investigation of dinuclear vanadium catalyst (R_a,*S*,*S*)-**10a** for homo-coupling of 4-hydroxycarbazoles will be discussed in (**Chapter 2**).

(ii) The catalytic enantioselective oxidative hetero-coupling of hydroxycarbazoles with 2-naphthol using a chiral mononuclear vanadium(V) complex has been developed for the first time. The coupling of hydroxycarbazole derivatives with various arenols provided axially chiral biarenols under mild conditions with high chemo-, regio-, and enantioselectivities. Interestingly, satisfactory functional group tolerance was achieved using mononuclear vanadium complexes. Moreover, the aerobic oxidative hetero-coupling with β-ketoesters also proceeded with high chemo- and stereoselectivities under slightly modified reaction conditions;[21] which will be discussed in (**Chapters 3 and 4**).

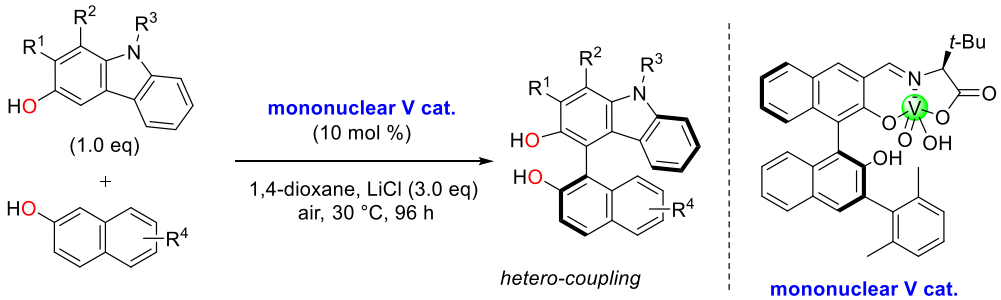

1.5 References:

1. Selected recent reviews and papers, see: (a) Wu, J.; Kozlowski, M. C. *ACS Catal.* **2022**, *12*, 6532−6549. (b) Zuo, Z, Kim, R. S.; Watson D. A. *J. Am. Chem. Soc*. **2021**, *143*, 1328−1333. (c) Bansal, S.; Shabade, A. B.; Punjia, P. *Adv. Synth. Catal.* **2021**, *363*, 1998– 2022. (d) Min, X.-L.; Zhang, X.-L.; Shen, R.; Zhang, Q.; He, Y. *Org. Chem. Front.* **2022**, *9*, 2280−2292. (e) Saito, T.; Shimizu, Y.; Araki, Y.; Ohgami, Y.; Kitazawa, Y.; Nishii, Y. *Eur. J. Org. Chem.* **2022**, e202101213. (f) Liu, C.-X.; Zhang, W.-W.; Yin, S.-Y.; Gu, Q.; You, S.-L, *J. Am. Chem. Soc.* **2022**, DOI: 10.1021/jacs.1c07635. (g) Carmona, J. A.; Rodríguez-Franco, C.; Fernández, R.; Hornillos, V.; Lassaletta, J. M. *Chem. Soc. Rev.* **2021**, *50*, 2968−2983. (h) Zhao, Q.; Peng, C.; Wang, Y.-T.; Zhan, G.; Han, B. *Org. Chem. Front.* **2021**, *8*, 2772−2785.
2. Christie, G. H.; Kenner, J. LXI. . *J. Chem. Soc., Trans.* **1922**, *121*, 614−620.
3. Selected recent reviews, see (a) Su, B.; Hartwig, J. F. *Angew. Chem. Int. Ed.* **2022**, *61*, e202113343. (b) Zhang, X.-X.; Zhang, Y.; Liao, L.; Gao, Y.; Su, H. E. M.; Yu, J.-S. *Chem. Cat. Chem.* **2022**, *14*, e202200126. (c) Sawano, T.; Takeuchi, R. *Catal. Sci. Technol.* **2022**, DOI: 10.1039/d2cy00316c. (d) Wang, X.; Chen, X.; Lin, W.; Li, P.; Li, W. *Adv. Synth. Catal.* **2022**, *364*, 1212−1222.
4. (a) Kumagai, N.; Kanai, M.; Sasai, H. A Career in Catalysis: Masakatsu Shibasaki, *ACS Catal.* **2016**, *6*, 4699–4709. (b) Xu, Y.; Kaneko, K.; Kanai, M.; Shibasaki, M.; Matsunaga, S. *J. Am. Chem. Soc.* **2014**, *136*, 9190−9194.
5. (a) Inukai, T.; Kano, T.; Maruoka, K. *Org. Lett.* **2021**, *23*, 792−796. (b) Pawliczek, M.; Hashimoto, T.; Maruoka, K. *Chem. Sci.* **2018**, *9*, 1231−1235. (c) Maruoka, K. Practical *Org. Process Res. Dev.* **2008**, *12*, 679−697.
6. (a) Banerjee, A.; Saha, S.; Maji, M. S. *J. Org. Chem.* **2022**, *87*, 4343−4359. (b) Liu, Y.; Wang, L.; Zhao, L.; Zhang, Y. Structure, *Nat. Prod. Rep*. **2022**, DOI: 10.1039/d1np00080b. (c) Tajuddeen, N.; Bringmann, G. *Nat. Prod. Rep*. **2021**, *38*, 2154−2186. (d) Moore, M. J.; Qu, S.; Tan, C.; Cai, Y.; Mogi, Y.; Keith, D. J.; Boger, D. L., *J. Am. Chem. Soc.* **2020**, *142*, 16039−16050. (e) Cao, N.; Chen, Y.; Ma, X.; Zeng, K.; Zhao, M.; Tu;.; Li, J.; Jiang, Y. *Phytochemistry* **2018**, *151*, 1−8.
7. (a) Phillips, A. M. F.; da Silva, M. de F. C. G.; Pombeiro, A. J. L. *Catalysts* **2020**, *10*, 529. (b) Sako, M.; Takizawa, S.; Sasai, H. *Tetrahedron* **2020**, *76*, 131645. (c) Pellissier, H. *Coord. Chem. Rev.* **2020**, *418*, 213395. (d) Grzybowski, M.; Sadowski, B.; Butenschön, H.; Gryko, D. T.. *Angew. Chem. Int. Ed.* **2020**, *59*, 2998−3027. (e) Tkachenko, N. V.; Bryliakov, K. P. *Mini-Reviews Org. Chem.* **2019**, *16*, 392−398. (f) Shalit, H. Dyadyuk, A.; Pappo, D. *J. Org. Chem*. **2019**, *84*, 1677−1686. (g) Wang, H. *Chirality* **2010**, *22*, 827−837. (h) Takizawa, S.

Chem. Pharm. Bull. **2009**, *57*, 1179−1188. (i) Kozlowski, M. C.; Morgan, B. J.; Linton, E. C. *Chem. Soc. Rev.* **2009**, *38*, 3193–3207. (j) Takizawa, S.; Katayama, T.; Sasai, H. *Chem. Commun.* **2008**, 4113−4122.

8. Representative examples of the metal-catalyzed highly enantioselective oxidative coupling of 2-naphthols, see (a) Smrcina, M.; Polakova, J.; Vyskocil, S.; Kocovsky, P. *J. Org. Chem.* **1993**, *58*, 4534−4538. (b) Nakajima, M.; Miyoshi, I.; Kanayama, K.; Hashimoto, S.-i.; Noji, M.; Koga, K. *J. Org. Chem.* **1999**, *64*, 2264−2271. (c) Irie, R.; Masutani, K.; Katsuki, T. *Synlett* **2000**, 1433−1436. (d) Li, X.; Yang, J.; Kozlowski, M. C. *Org. Lett.* **2001**, *3*, 1137−1140. (e) Barhate, N. B.; Chen, C.-T. *Org. Lett.* **2002**, *4*, 2529–2532. (f) Chu, C.-Y.; Uang, B.-J. *Tetrahedron: Asymmetry* **2003**, 14, 53–55. (g) Tada, M.; Taniike, T.; Kantam, L. M.; Iwasawa, Y. *Chem. Commun.* **2004**, 2542−2543. (h) Kim, K. H.; Lee, D.-W.; Lee, Y.-S.; Ko, D.-H.; Ha, D.-C. *Tetrahedron* **2004**, *60*, 9037−9042. (i) Habaue, S.; Murakami, S.; Higashimura, H. *J. Polym. Sci., Part A: Polym. Chem.* **2005**, *43*, 5872−5878. (j) Temma, T.; Habaue, S. *J. Polym. Sci., Part A: Polym. Chem.* **2005**, *43*, 6287−6294. (k) Alamsetti, S. K.; Poonguzhali, E.; Ganapathy, D.; Sekar, G. *Adv. Synth. Catal.* **2013**, *355*, 2803−2808. (l) Zhang, Q.; Cui, X.; Chen, L.; Liu, H.; Wu, Y. *Eur. J. Org. Chem*. **2014**, 7823−7829. (m) Prause, F.; Arensmeyer, B.; Fröhlich, B.; Breuning, M. *Catal. Sci. Technol.* **2015**, ***5***, 2215−2226. (n) Mandal, M.; Nagaraju, V.; Karunakar, G. V.; Sarma, B.; Borah, B. J.; Bania, K. K. *J. Phys. Chem.* **2015**, *119*, 28854−28870. (o) Narute, S.; Parnes, R.; Toste, F. D.; Pappo, D. *J. Am. Chem. Soc.* **2016**, *138*, 16553−16560. (p) Dyadyuk, A.; Vershinin, V.; Shalit, H.; Shalev, H.; More, N. Y.; Pappo, D. *J. Am. Chem. Soc.* **2022**, *144*, 3676–3684. (q) Horibe, T.; Nakagawa, K.; Hazeyama, T.; Takeda, K.; Ishihara, K. *Chem. Commun*. **2019**, *55*, 13677–13680. (r) Tian, J.-M.; Wang, A.-F.; Yang, J.-S.; Zhao, X.-J.; Tu, Y.-Q.; Zhang, S.-Y.; Chen, Z.-M. *Angew. Chem. Int. Ed.* **2019**, *58*, 11023–11027. (s) Zhao, X.-J.; Li, Z.-H.; Ding, T.-M.; Tian, J.-M.; Tu, Y-.Q.; Wang, A.-F.; Xie, Y.-Y. *Angew. Chem. Int. Ed.* **2021**, *60*, 7061–7065. (t) Hayashi, H.; Ueno, T.; Kim, C.; Uchida, T. *Org. Lett.* **2020**, *22*, 1469–1474. (u) Wang, P.; Cen, S.; Gao, J.; Shen, A.; Zhang, Z. *Org. Lett.* **2022**, *24*, 2321–2326. (v) Luo, Z.; Liu, Q.; Gong, L.; Cui, X.; Mi, A.; Jiang, Y. *Chem. Commun*. **2002**, 914−915. (w) Gao, J.; Reibenspies, J. H.; Martell, A. E. *Angew. Chem., Int. Ed.* **2003**, *42*, 6008−6012. (x) Egami, H.; Katsuki, T. *J. Am. Chem. Soc.* **2009**, *131*, 6082−6083.

9. Kim, H. Y.; Takizawa, S.; Sasai, H.; Oh, K. *Org. Lett.* **2017**, *19*, 3867–3870.

10. Somei, H.; Asano, Y.; Yoshida, T.; Takizawa, S.; Yamataka, H.; Sasai, H. *Tetrahedron Lett*. **2004**, *45*, 1841−1844. (b) Takizawa, S.; Katayama, T.; Kameyama, C.; Onitsuka, K.; Suzuki, T.; Yanagida, T.; Kawai, T.; Sasai, H. *Chem. Commun.* **2008**, 1810−1812. (c) Sako, M.;

Aoki, T.; Zumbrägel, N.; Schober, L.; Gröger, H.; Takizawa, S.; Sasai, H. *J. Org. Chem.* **2019**, *84*, 1580−1587.

11. Selected reviews: (a) Jabir, N. R.; Firoz, C. K.; Bhushan, A.; Tabrez, S.; Kamal, M. A. *Anti-cancer Agents in Med. Chem.* **2018**, *18*, 6.
12. Dubois, M.-A.; Grandbois, A.; Collins, S. K.; Schmitzer, A. R.; *J. Mol. Recognit*. **2011**, *24*, 288.
13. Brütting, C.; Fritsche, R. F.; Kutz, S. K.; Börger, C.; Schmidt, A. W.; Kataeva, O.; Knölker, H.-J. *Chem. Eur. J.* **2018**, *24*, 458.
14. Tasler, S.; Bringmann, G. *Chem. Rec.* **2002**, *2*, 113
15. Moody, C. J.; Shah, P. *J. Chem. Soc., Perkin Trans.* **1989**, *1*, 2463.
16. (a) Bringmann, G.; Ledermann, A.; Stahl, M.; Gulden, K.-P. *Tetrahedron* **1995**, *51*, 9353. (b) Lin, G.; Zhang, A. *Tetrahedron* **2000**, *56*, 7163. (c) Fillion, H.; Bouaziz, Z.; Nebois, P.; Poumaroux, A. *Heterocycles* **2000**, *52*, 977.
17. Knölker, H.-J.; Goesmann, H.; Hofmann, C. *Synlett* **1996**, 737.
18. (a) Liu, L.; Carroll, P. J.; Kozlowski, M. C. *Org. Lett.* **2015**, 17, 508. (b) Kang, H.; Lee, Y. E.; Reddy, P. V. G.; Dey, S.; Allen, S. E.; Niederer, K. A.; Sung, P.; Hewitt, K.; Torruellas, C.; Herling, M. R.; Kozlowski, M. C. *Org. Lett*. **2017**, *19*, 5505. (c) Kang, H.; Herling, M. R.; Niederer, K. A.; Lee, Y. E.; Reddy, P. V. G.; Dey, S.; Allen, S. E.; Sung, P.; Hewitt, K.; Torruellas, C.; Kim, G. J.; Kozlowski, M. C. *J. Org. Chem*. **2018**, *83*, 14362.
19. Sako, M.; Sugizaki, A.; Takizawa, S. *Bioorg. Med. Chem. Lett.* **2018**, *28*, 2751
20. Kamble, G. T.; Salem, M. S. H.; Abe, T.; Park, H.; Sako, M.; Takizawa, S.; Sasai, H. *Chem. Lett*. **2021**, *50*, 1755.
21. Sako, M.; Higashida, K.; Kamble, G. T.; Kaut, K.; Kumar, A.; Hirose, Y.; Zhou, D.; Suzuki, T.; Rueping, M.; Maegawa, T.; Takizawa, S.; Sasai, H. *Org. Chem. Front.* **2021**, *8*, 4878.
22. Li, X.; Hewgley, J. B.; Mulrooney, C. A.; Yang, J.; Kozlowski, M. C. *J. Org. Chem.* **2003**, *68*, 5500.
23. (a) Habaue, S.; Takahashi, Y.; Temma, T. *Tetrahedron Lett.* **2007**, *48*, 7301. (b) Temma, T.; Hatano, B.; Habaue, S. *Tetrahedron* **2006**, *62*, 8559. (c) Temma, T.; Habaue, S. *Tetrahedron Lett.* **2005**, *46*, 5655.
24. Tian, J.-M.; Wang, A.-F.; Yang, J.-S.; Zhao, X.-J.; Tu, Y.-Q.; Zhang, S.-Y.; Chen, Z.-M. *Angew. Chem. Int. Ed.* **2019**, *58*, 11023.
25. Egami, H.; Matsumoto, K.; Oguma, T.; Kunisu, T.; Katsuki, T. *J. Am. Chem. Soc.* **2010**, *132*, 13633.

Chapter 2

Enantioselective Homo-coupling of 4-Hydroxycarbazole

Chiral vanadium complexes are proven as effective catalysts for the synthesis of homo-coupling of 2- and 3-hydroxycarbazoles. The recent reports by Kozlowski and our research group successfully demonstrated the utility of these complexes. This chapter will be focused on the first stereoselective oxidative homo-coupling of 4-hydroxycarbazoles using a chiral vanadium catalyst.

2.1 Synthesis of 4-Hydaroxycarbazole Precursor

The synthesis of the 4-hydaroxycarbazole precursor was achieved by using readily available starting material 2-Bromo nitrobenzene as shown in (**Scheme 6**).

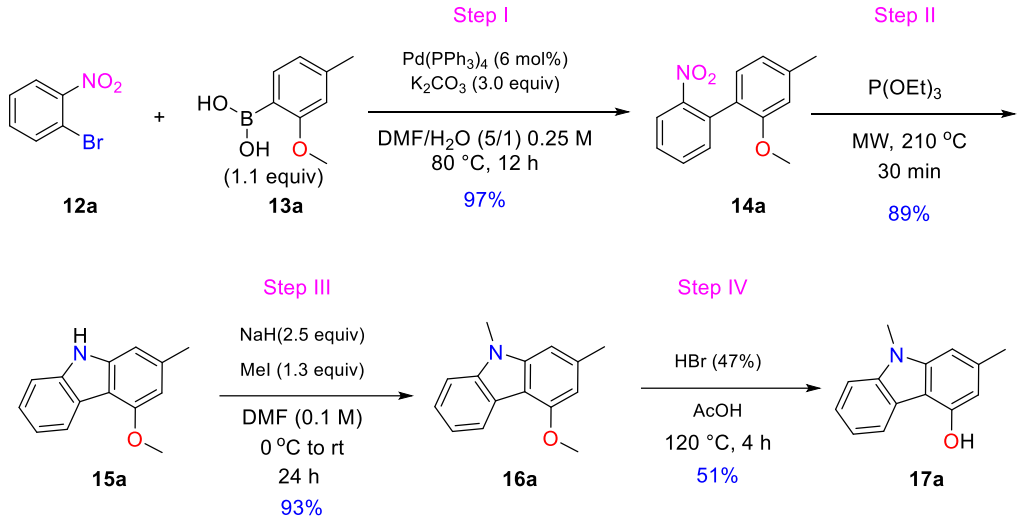

Scheme 6. General synthetic route of 4-hydraoxycarbazole derivatives.

The commercially available **12a** and **13a** (1.1 eq.) were reacted under the Suzuki-Miyaura coupling conditions to afford **14a** in 97% yield as a light-yellow solid.[28] The **14a** was then subjected to cyclization using the Cadogan cyclization method to afford **15a** in 89% yield.[29] Subsequently, the methoxy intermediate **15a** was protected using an appropriate methylated agent (step III) to give **16a** in 93% yield.[30] Lastly, the methoxy deprotection of **16a** was carried out under HBr (47%) in AcOH at 120 °C to afford **17a** as a white solid.[18a]

2.2 Screening of Vanadium Catalyst for Homo-coupling

Various vanadium-based catalysts were screened for the homo-coupling reaction of hydroxy carbazole **17a**. The homocoupling of **17a** with mononuclear vanadium(V) catalysts (*S*)-**4c** and (R_a,*S*)-**8b** delivered up to 25 % yield and up to 25 % ee. The vanadium(V) complex

(R_a,*S*,*S*) contains an axial chirality of the (*R*)-BINOL skeleton and two central chirality of (*S*)-amino acids. The utilization of a diastereomeric catalyst (S_a,*S*,*S*)-**10a** gave **18a** in 66% yield with 51% ee, suggesting that the (R_a,*S*,*S*) catalyst **10a** represents the matched pair and the (S_a,*S*,*S*) catalyst **10a** is the mismatched pair.

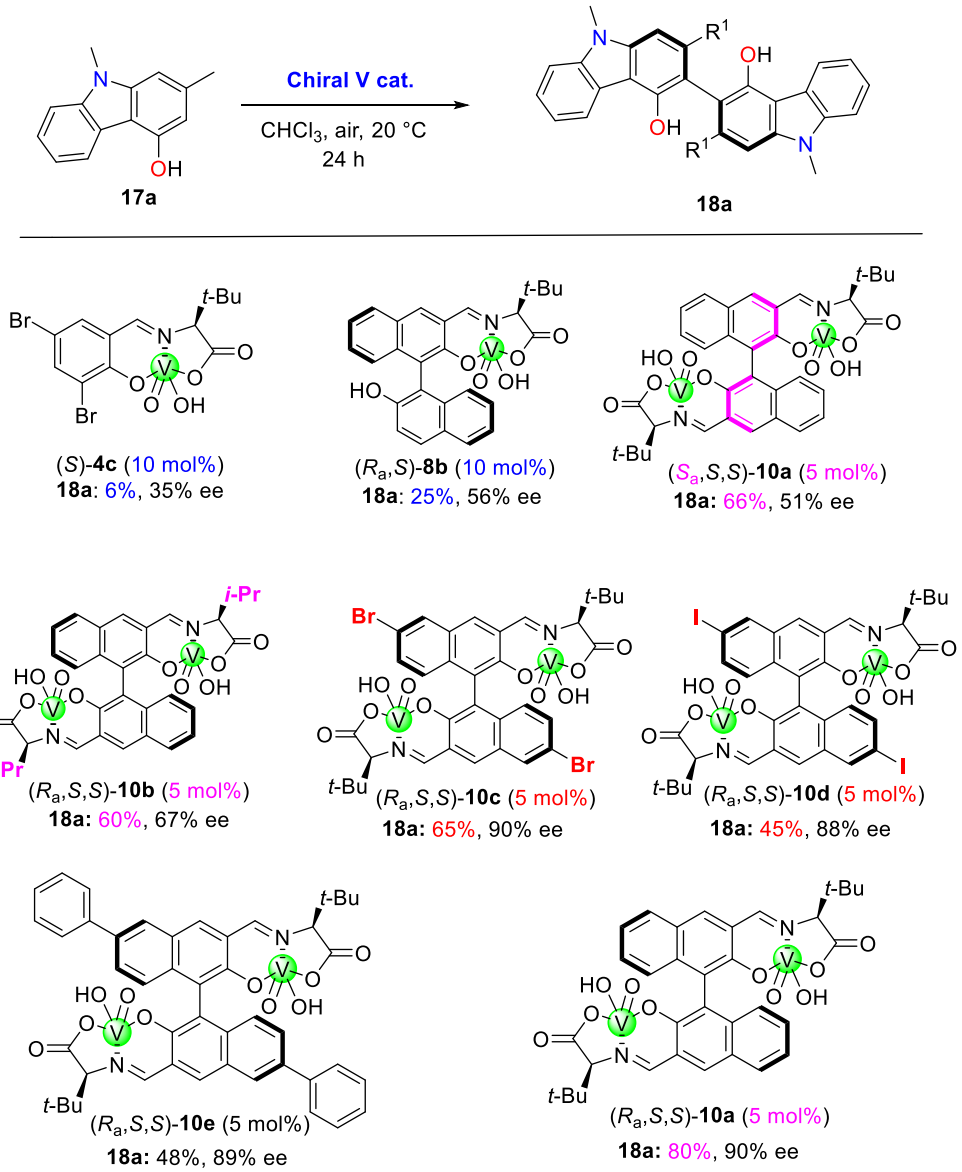

Table 1: Screening of chiral vanadium(V) catalysts for enantioselective oxidative coupling of **17a**

Neither the catalyst (R_a,*S*,*S*)-**10b** with an *iso*-propyl group instead of a *tert*-butyl group at the amino acid moiety nor the catalysts (R_a,*S*,*S*)-**10b, 10c, 10d** with Bromine and Iodine atom at 6,6'-position could illustrate lower yields, respectively. A bulky substituent (Ph group) introduced at the 6,6'-position of a BINOL skeleton[32] showed a considerable improvement in catalytic activity and enantioselectivity with 48% yield and 89% ee. (**Table 1**)

These different catalytic activities between mono- and di-nuclear vanadium(V) complexes could be ascribed to intermolecular or intramolecular manner coupling through a dual activation mechanism. In the dual activation mechanism, two substrates activate at the same time with the dinuclear vanadium complex. This concept has been reported by the Sasai group.[30] Finally, the screening of vanadium catalyst (R_a,*S*,*S*)-**10a** shows an overall good result of 80% yield with 90% ee. Also, the consumption of (R_a,*S*,*S*)-**10a** (5 mol%), lower amount of catalyst loading supports the mechanism of intramolecular coupling through a dual activation mechanism.

2.3 Optimization of Homo-coupling Reaction Conditions

The optimization of suitable reaction conditions for homocoupling of hydroxycarbazole was screened with vanadium(V) catalyst **10a** under different solvents and temperatures as shown in **Table 2.** The model substrate **17a** was subjected to homocoupling to obtain product leads to excellent yields as well enantioselectivity.

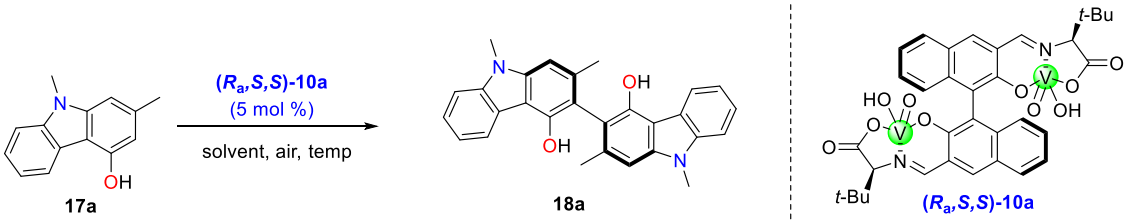

entry	solvent	temp.°C	time (h)	yield (%)[a]	ee (%)
1	Toluene	30	20	53	88
2	*O*-Xylene	30	24	50	82
3	Chlorobenzene	30	24	55	85
4	CH_2Cl_2	30	24	48	76
5	$(ClCH_2)_2$	30	22	63	87
6	$(Cl_2CH)_2$	30	19	62	87
7	$CHCl_3$	30	24	72	90
8	$CHCl_3$	20	24	**80**	**90**
9	$CHCl_3$	10	24	62	89

aDetermined by 1H NMR spectroscopy using 1,3,5-trimethoxybenzene as an internal standard

Table 2: Optimization of enantioselective oxidative coupling of **17a** using catalyst **10a**

Initially, the reaction was performed at 30 °C under air[31] in aromatic solvents such as toluene, *o*-xylene, and chlorobenzene (**Table 1**, entries 1-3). It was observed that the desired product **18a** was obtained in moderate yields (50-55 %) with high enantioselectivities (82-88 % ee). Subsequently, the halogenated solvents were explored (entries 4-7) and it was found that chloroform works smoothly for this reaction. The product **18a** was obtained in 72% yield with 90% ee (entry 7) due to less stability of **17a**. Furthermore, when the reaction temperature was lowered to 20 °C, the yield of **18a** was slightly increased to 80% with 90% ee (entry 8). However, the lower reaction temperature 10 °C led to a reduction in yield of **18a** (62%) while maintaining the high enantioselectivity of 89% ee (entry 9). Thus, were explored the substrate scope and limitations using catalyst **10a**, and chloroform as solvent at 20 °C.

2.4 Substrate Scope:

With the optimized reaction conditions in hand, we explored the substrate scope and limitations **(Table 3)**. A coupling of 1,2-dimethyl-*NH* substituted hydroxycarbazole **17b** quantitatively yielded the product **18b** in 80% ee due to its electron-rich nature. Also, 1,2- and *N*-trimethyl substituted hydroxycarbazole **17c** led to **18c** with good enantioselectivity (70% ee) and high yield (90%). The 1,2,7-Trimethyl-*NH*-substituted hydroxycarbazole starting material **17d** delivered **18d** with 88% yield and 90% ee. Similarly, when substrates **17e-h** possessing aryl, benzyl groups on the nitrogen atom were applied to the oxidative coupling reaction, the corresponding products **18e-h** were obtained in good yields (68-94%), albeit with lower enantioselectivities (56-76%). A massive group of nitrogen affected enantioselectivity due to the steric hindrance. Allyl substitution nitrogen **17i** delivered **18i** with a good yield of 75% but enantioselectivity dropped up to 46% might be π-π interaction affected.

The electron-withdrawing group on nitrogen **17j** as result could not obtain any product due to the less electron density on 4-hydroxycarbazole**.** The different verities of 2-hydroxycarbazole **2d** instead of 4- hydroxycarbazole **17** using optimized conditions have been screened. As result, the oxidative coupled product delivered in good yield but could not achieve good enantioselective due to its low racemization barrier.

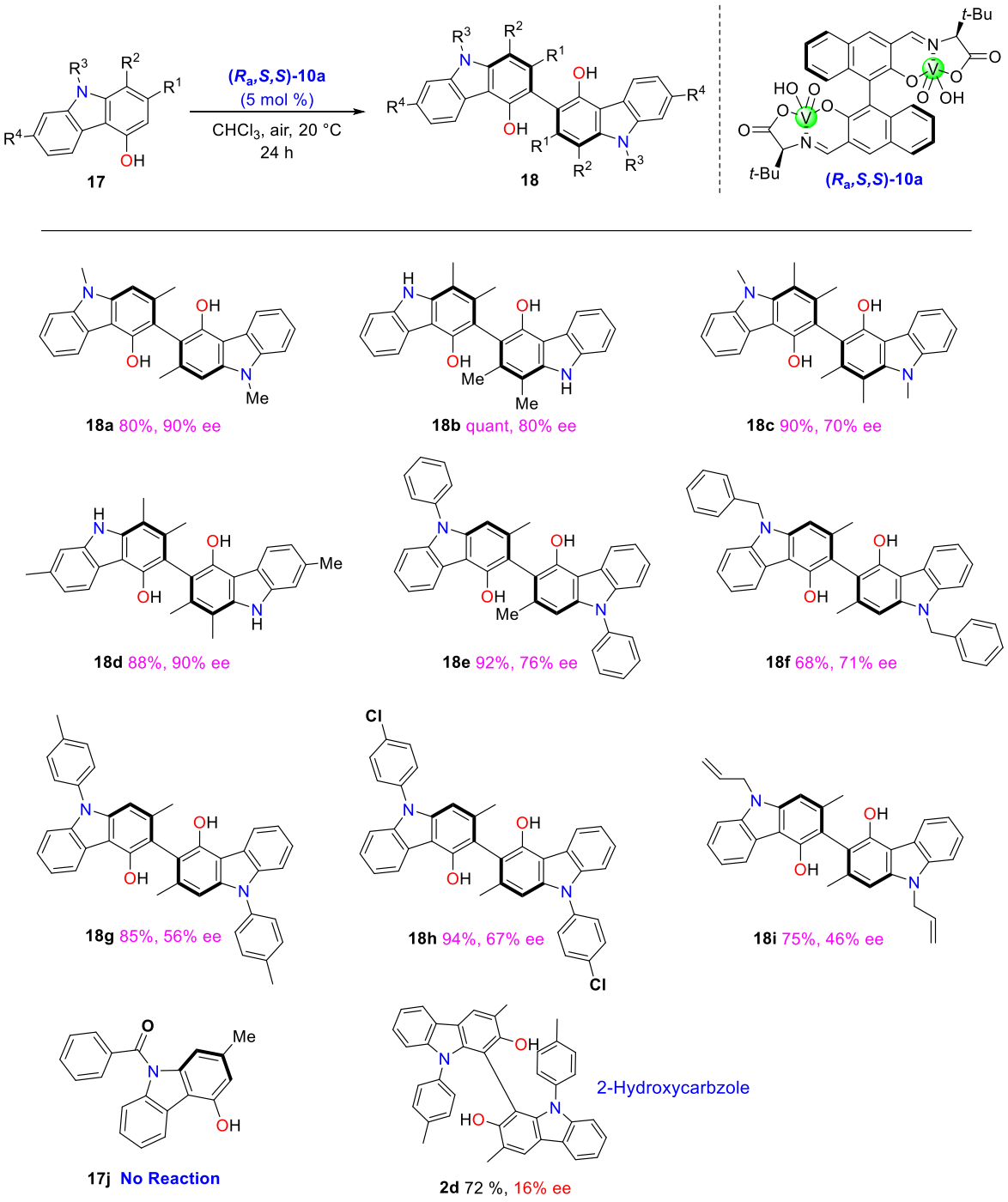

Table 3. Substrate Scope and Limitations

2.5 X-ray Crystallography of Coupling Product 18a:

The optically pure **18a** was readily accessible by single recrystallization of the enantioenriched product from DCM and hexane. The absolute configuration of **18a** is determined to be *S* based on the Flack parameter [0.04(7)] obtained *via* the X-ray

crystallographic analysis depicts that the product adopts (*S*)-form under optimal reaction conditions (**Scheme 7**).

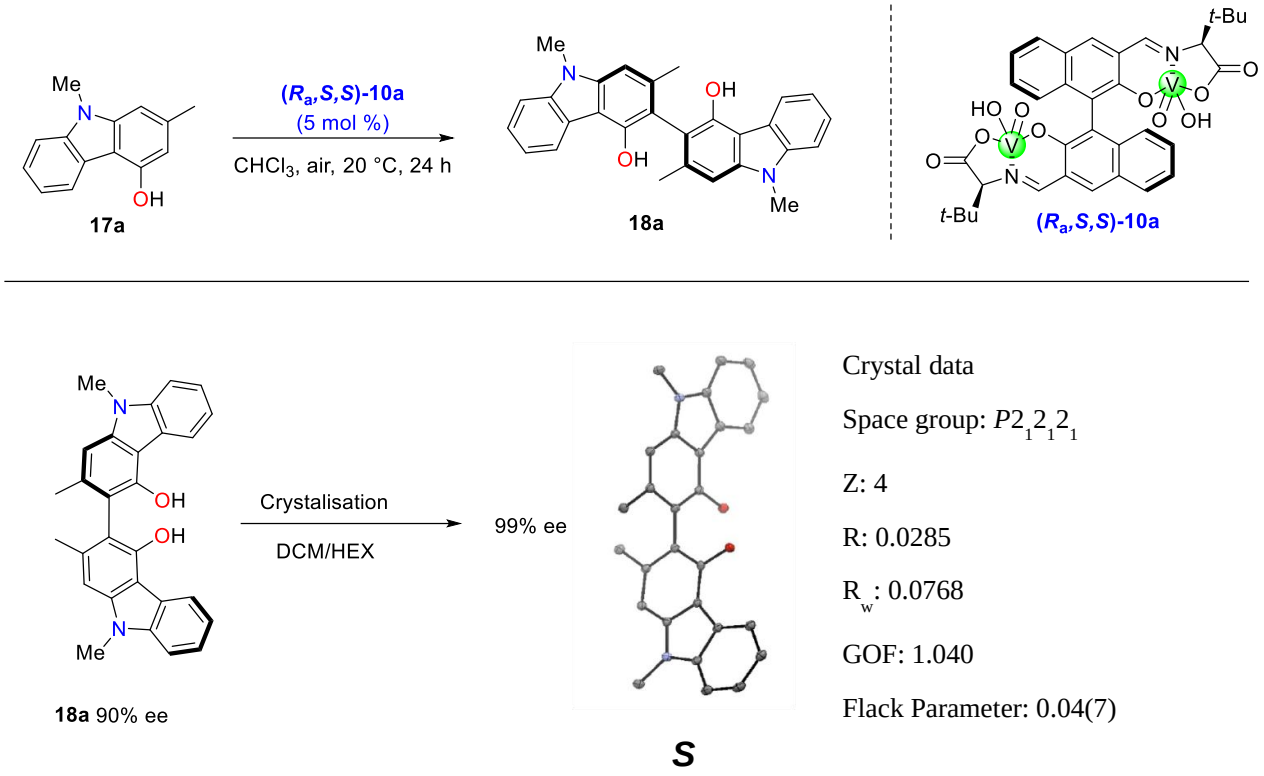

Scheme 7. X-ray Crystallographic Analysis for Absolute Configuration of **18a**

2.6 Axial Chiral Stability (DFT calculations)

The obtained single crystal data confirmed that atropisomerization occurs in **18a**, and the activation energies were quantified using density functional theory (B3LYP/D95**). Atropisomers should interconvert at a given temperature with a half-life of at least 1000 seconds, corresponding to an activation barrier of 22 kcal/mol at 27 °C.[33] The calculated activation energies hurdles for the racemization of **18a** at 27 °C are 69.0 and 29.2 kcal/mol, (**Figure S1**), indicating the potential functionality of the biaryl frameworks **18** as C_2-symmetric chiral ligands for asymmetric catalysis.[34]

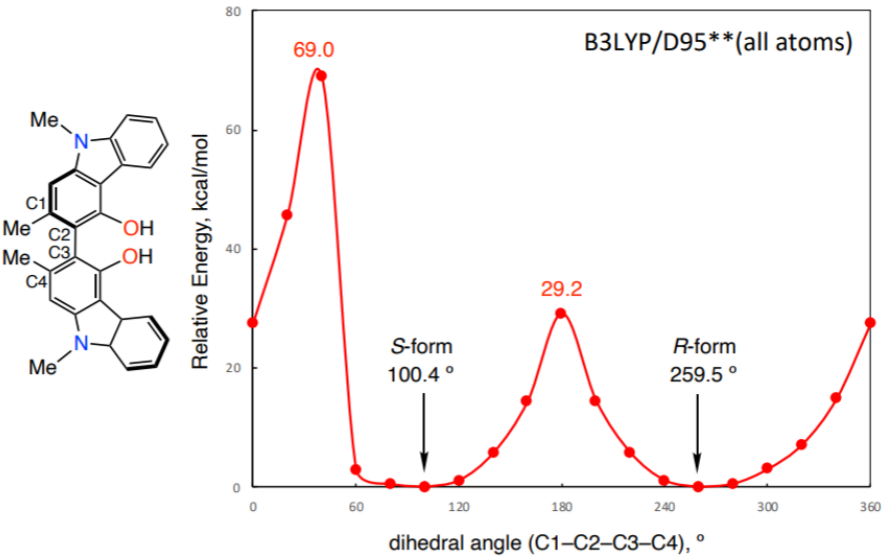

Figure. S1a The activation energy for the conversion from *S*-form to *R*-form.

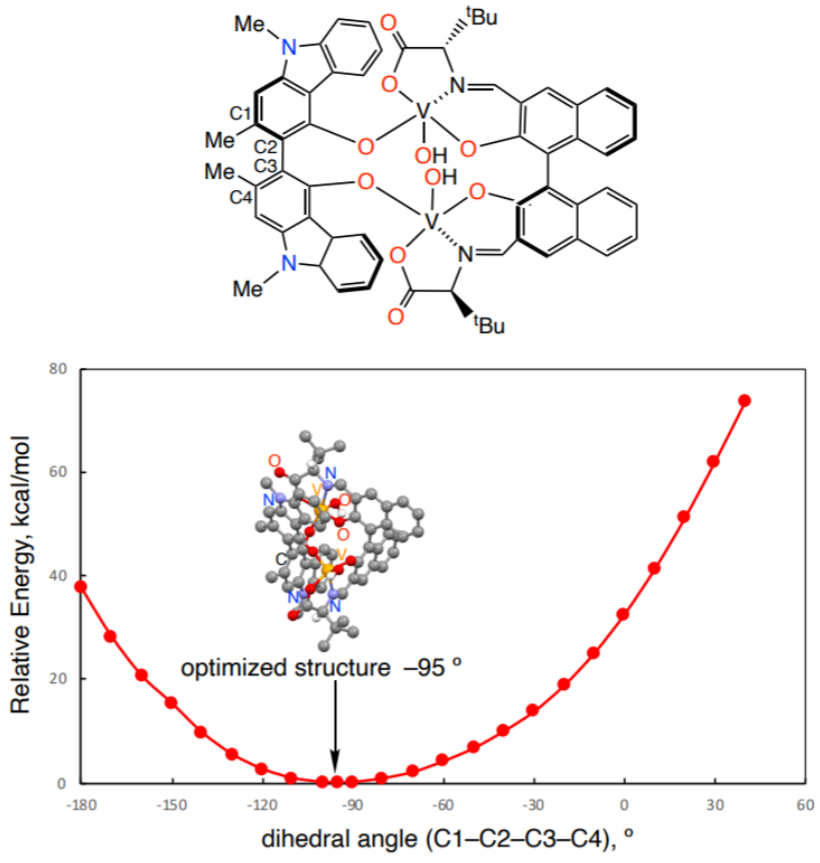

Figure. S1b Plots of the relative energy against the dihedral angle (C1–C2–C3–C4)

2.7 Proposed Reaction Mechanism:

Previously, our group has reported using dinuclear vanadium complex (R_a,*S*,*S*)-**10a** to catalyse the oxidative coupling of 2-naphthols to the corresponding (*S*)-BINOL derivatives in

excellent yields with up to 97% ee through a dual activation mechanism.[36] The chiral dinuclear vanadium(V) complex (R_a,*S*,*S*)-**10a** with two identical metal centres in a 1,1'-bi-2-naphthol (BINOL) backbone could simultaneously activate two substrates in a homolytic radical-radical coupling reaction of hydroxycarbazole molecules, would do this increase the reaction rate as well with high enantioselectivity.

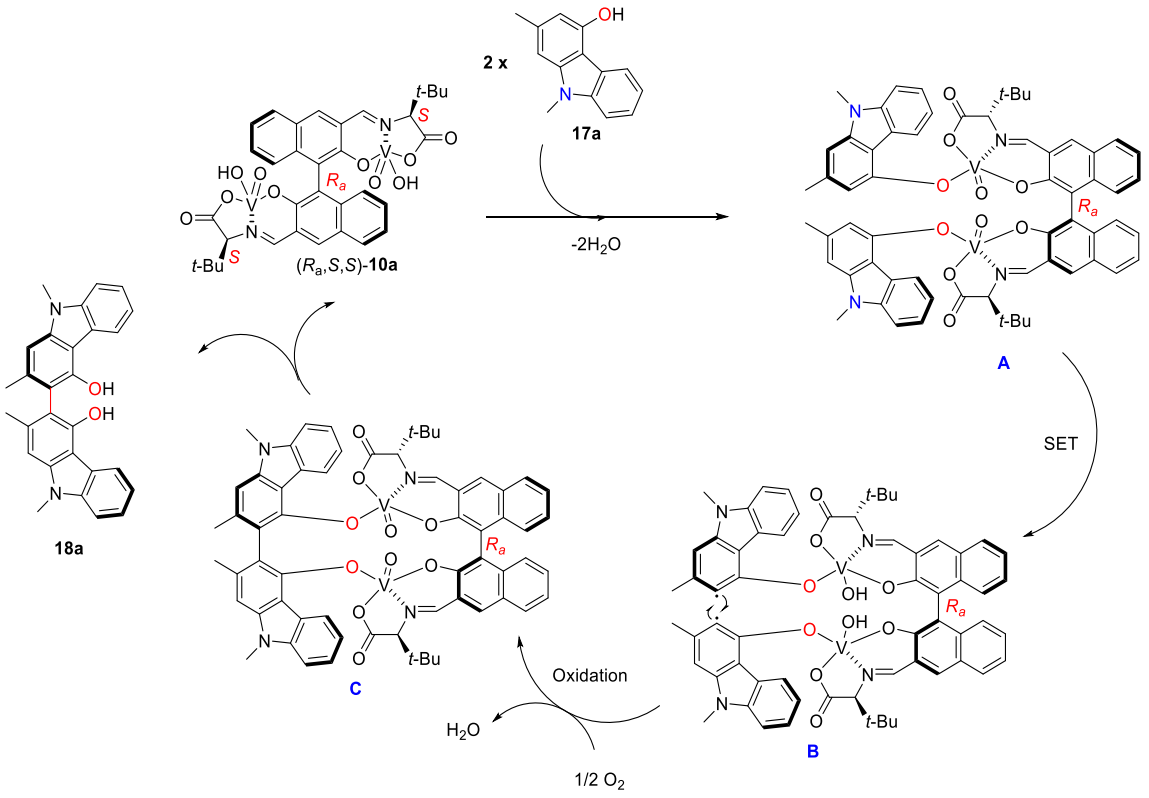

Scheme 8. Enantioselective coupling of 4-hydroxycarbazoles *via* dual activation mechanism

First, each vanadium (V) atom of the complex (R_a,*S*,S)-**10a** binds to a molecule of 4-hydroxycarbazole **17** to provide intermediate **A** (**Scheme 8**). The carbazole-containing hydroxy group approaches the vanadium atom from the opposite side of the bulky *t*-butyl group, and the methyl group on carbazole **17** positions itself far away from the *t*-butyl group due to the steric repulsion, aligning two molecules of **18** in *S* conformation. The C-C bond formation followed by a single electron transfer from carbazole to vanadium (V) results in radical formation **B** and intermediate **C**. The coupling product **18** is released in *S*-form and the vanadium complex is re-oxidated by the existence of molecular oxygen in the air to lead intermediate **A** to proceed to the catalytic cycle.

The formation of intermediate **B** to intermediate **C** is the enantio-determining step. Two carbazole molecules hold by a vanadium catalyst at the same time resulted in C-C bond formation with the preferred *S* configuration as shown in (**Figure. S2**). The steric effects between the carbazole and vanadium complex play an important role in the stereochemical output. The *R* configuration is unfavourable as two carbazole molecules coordinate with the vanadium complex but get repelled due to carbonyl groups present on the catalyst.

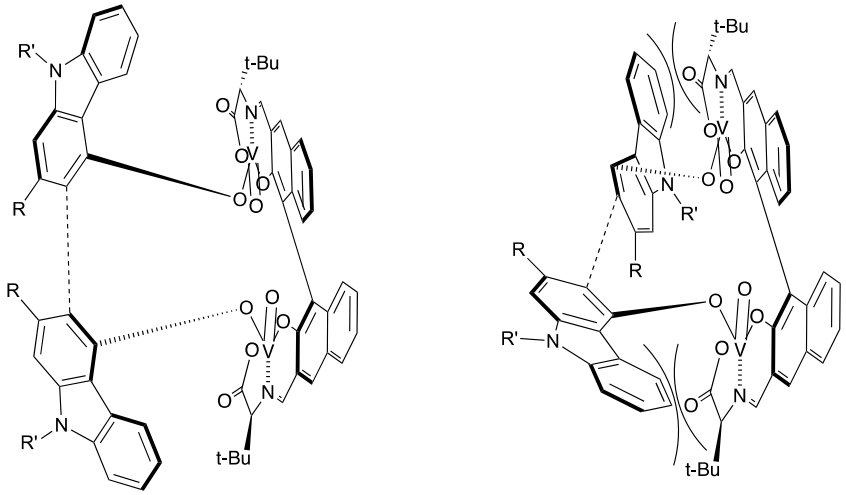

Favourable from **B** to **C**
"*S*" form

unfavourable from **B** to **C**
"*R*" form

Figure. S2 Configurational Alignment

In summary, I successfully developed the first protocol for the highly enantioselective oxidative homo-coupling of 4-hydroxycarbazoles to synthesize axially chiral dimeric hydroxycarbazoles. The chiral dinuclear vanadium(V) complex showed high catalytic activity owing to its dual initiation of hydroxycarbazoles by dinuclear vanadium complex **10a**

2.8 Experimental Section:

^{1}H-, and ^{13}C-NMR were recorded with JEOL JMN ECS400 FT NMR, or Bruker AVANCE II (^{1}H-NMR 400 MHz, ^{13}C-NMR 100 MHz) ^{1}H-NMR spectra are reported as follows: a chemical shift in ppm downfield of tetramethylsilane (TMS) and referenced to residual solvent peak ($CDCl_3$) at 7.26 ppm, or ($(CD_3)_2CO$) at 2.05 ppm, integration, multiplicities (*s* = singlet, *d* = doublet, *t* = triplet, *q* = quartet, *m* = multiplet), and coupling constants (Hz). ^{13}C-NMR spectra were reported in ppm relative to the central line of triplet for

$CDCl_3$ at 77.16 ppm, or the central line of septet for ($(CD_3)_2CO$) at 29.84 ppm. ESI-MS spectra were obtained with JMS-T100LC (JEOL). Optical rotations were measured with a JASCO P-1030 polarimeter. HPLC analyses were performed on a JASCO HPLC system (JASCO PU 980 pump and UV-975 UV/Vis detector) using a mixture of hexane and 2-propanol as eluents. FT-IR spectra were recorded on a JASCO FT-IR system (FT/IR4100). Thin-layer chromatography (TLC) analysis of reaction mixtures was performed using Merck silica gel 60 F254 TLC plates and visualized under UV. Column chromatography on SiO_2 was performed with Kanto Silica Gel 60 (63-210 μm). Melting points were determined with a Melting Point Apparatus MP-S9 (Yanaco, Japan) and were uncorrected. Chiral vanadium(v) catalysts **10a-e** were synthesized and confirmed according to our previously reported method.[37] Commercially available organic and inorganic compounds were used without further purification.

Synthesis of Substrates:

2-Methoxy-4-methyl-2'-nitro-1,1'-biphenyl (14a)

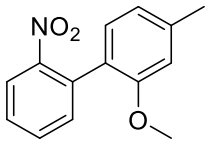

In a dry round bottom flask, (2-methoxy-4-methyl phenyl) boronic acid **13a** (1.1 equiv), K_2CO_3 (3.0 equiv), and $Pd(PPh_3)_4$ (6 mol%) were dissolved in DMF and H_2O (DMF/H_2O = 5/1, 0.25 M). Then, 1-Bromo-2-nitrobenzene **12a** (1.0 equiv) was added portion-wise under nitrogen, and the resulting mixture was heated up to 80 °C, overnight. The reaction was quenched after completion and the product was extracted with EtOAc (3 times), dried over Na_2SO_4, and concentrated under reduced pressure. The residue was purified by silica column chromatography (*n*-Hexane/EtOAc = 5/1) to afford the desired product 2-methoxy-4-methyl-2'-nitro-1,1'-biphenyl **14a** in 97% yield as light-yellow solid.

^{1}H NMR (400 MHz, $CDCl_3$): δ 7.91 (dd, J = 8.1, 1.0 Hz, 1H), 7.61 (ddd, J = 7.8, 7.3, 1.4 Hz, 1H), 7.44(ddd, J = 8.0, 7.6, 1.4 Hz, 1H), 7.40 (dd, J = 7.8, 1.4 Hz, 1H), 7.20 (d, J = 7.3 Hz, 1H), 6.90 (d, J = 6.9 Hz, 1H), 6.73 (s, 1H), 3.69 (s, 3H), 2.41 (s, 3H).

^{13}C NMR (100 MHz, $CDCl_3$): δ 155.85, 149.92, 140.28, 133.26, 132.74, 132.61, 129.57, 127.90, 124.24, 123.99, 122.04, 111.77, 55.23, 21.86.

HRMS (ESI): calcd for $C_{14}H_{13}NO_3$: *m/z* 244.0968 $[M + H]^+$, found 244.0962.

IR (KBr): 2993, 2971, 2941, 1865, 1615, 1580, 1462, 1356, 819, 734 cm^{-1}.

mp: 80-82 °C.

4-Methoxy-2-methyl-*9H*-carbazole (15a)

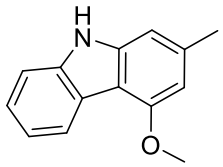

In a dry microwave reaction tube, 2-methoxy-4-methyl-2'-nitro-1,1'-biphenyl **14a** was dissolved in $P(OEt)_3$ (0.3 M) and stirred at 210 °C for 30 min in a microwave reactor. After the elapsed time, the reaction mixture was concentrated under reduced pressure. The residue was purified by silica column chromatography (*n*-Hexane/EtOAc = 7/1) to afford the desired product 4-methoxy-2-methyl-*9H*-carbazole **15a** in 89% yield as a brown solid.

^{1}H NMR (400 MHz, $CDCl_3$): δ 8.31 (d, J = 7.8 Hz, 1H), 7.74 (s, 1H), 7.38 (dd, J = 8.3, 6.9 Hz, 1H), 7.24-7.31 (m, 2H), 6.74 (s, 1H), 6.53 (s, 1H), 4.07 (s, 3H), 2.53 (s, 3H).

^{13}C NMR (100 MHz, $CDCl_3$): δ 155.99, 141.30, 138.79, 137.30, 124.50, 122.84, 122.69, 119.62, 110.49, 110.01, 103.82, 102.18, 55.45, 22.55.

HRMS (ESI): calcd for $C_{14}H_{14}NO$: *m/z* 212.1070 $[M + H]^+$, found 212.1068.

IR (KBr): 3381, 3053, 2968, 2842, 1582, 1454, 1349, 1209, 809, 746 cm^{-1}.

mp: 105-107 °C.

4-Methoxy-2,9-dimethyl-*9H*-carbazole (16a)

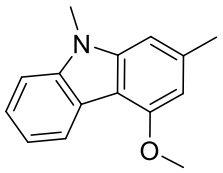

To a stirring solution of DMF (0.1 M) and NaH (2.5 equiv) was added a solution of **15a** (1.0 equiv) at 0 °C. After stirring for 10 minutes at room temperature, iodomethane (1.3 equiv) was added to the solution and the reaction mixture was allowed to stir at r.t for 24 h, then it was cooled to 0 ºC and water was added. The mixture was extracted with EtOAc (3 times). The combined organic layers were washed with brine, dried over anhydrous Na_2SO_4, filtered, and evaporated *in vacuo*. The crude product was purified by silica-gel column chromatography to afford **16a** as a white solid in a 93% yield.

^{1}H NMR (400 MHz, $CDCl_3$): δ 8.37 (d, J = 7.3 Hz, 1H), 7.48 (ddd, J = 7.8, 7.3, 1.4 Hz, 1H), 7.38 (d, J = 8.2 Hz, 1H), 7.31 (ddd, J = 7.8, 7.3, 1.4 Hz, 1H), 6.87 (s, 1H), 6.57 (s, 1H), 4.11 (s, 3H), 3.80 (s, 3H), 2.63 (s, 3H).

^{13}C NMR (100 MHz, $CDCl_3$): δ 155.97, 142.80, 140.31, 137.04, 124.24, 122.62, 122.33, 119.05, 109.70, 107.83, 101.79, 101.73, 55.43, 29.20, 22.77.

HRMS (ESI): calcd for $C_{15}H_{15}NO$: *m/z* 248.1154 $[M + Na]^+$, found 248.1145.

IR (KBr): 3068, 2943, 2844, 1628, 1600, 1469, 1414, 1326, 1227, 1107, 1046, 805, 745 cm^{-1}.

mp: 125-127 °C.

2,9-Dimethyl-*9H*-carbazol-4-ol (17a)

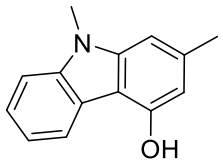

In a dry round bottom flask, compound **16a** was dissolved in AcOH (0.16 M) under an N_2 atmosphere at room temperature. The reaction mixture was refluxed at 120 °C for 15 min, then (HBr, 47%) (20 equiv) was added dropwise over 10 min. The reaction was refluxed for 4 h, then diluted with water (30 ml) to quench the reaction after completion, and the desired product was extracted with EtOAc (3 times). Organic layers were dried over Na_2SO_4, concentrated *in vacuo*, and purified by column chromatography on silica gel (*n*-Hexane/EtOAc = 5/1) to afford **17a** as a brown solid in 51% yield.

^{1}H NMR (400 MHz, $(CD_3)_2CO$)): δ 8.92 (s, 1H), 8.26 (d, J = 7.8 Hz, 1H), 7.41 (d, J = 8.2 Hz, 1H), 7.36 (t, J = 7.3 Hz, 1H), 7.16 (t, J = 7.3 Hz, 1H), 6.82 (s, 1H), 6.54 (s, 1H), 3.79 (s, 3H), 2.45 (s, 3H).

^{13}C NMR (100 MHz, $(CD_3)_2CO$): δ 154.09, 144.22, 141.29, 137.60, 124.82, 123.31, 123.04, 119.45, 109.78, 108.75, 106.86, 101.47, 29.27, 22.32.

HRMS (ESI): calculated for $C_{14}H_{14}NO$: *m/z* 212.1070 $[M + H]^+$, found 212.1067.

IR (KBr): 3491, 2921, 1639, 1604, 1470, 1327, 1268, 1130, 803, 744 cm^{-1}.

mp: 185-187 °C.

Enantioselective oxidative coupling of 4-hydroxycarbazoles (17) to synthesize products (18)

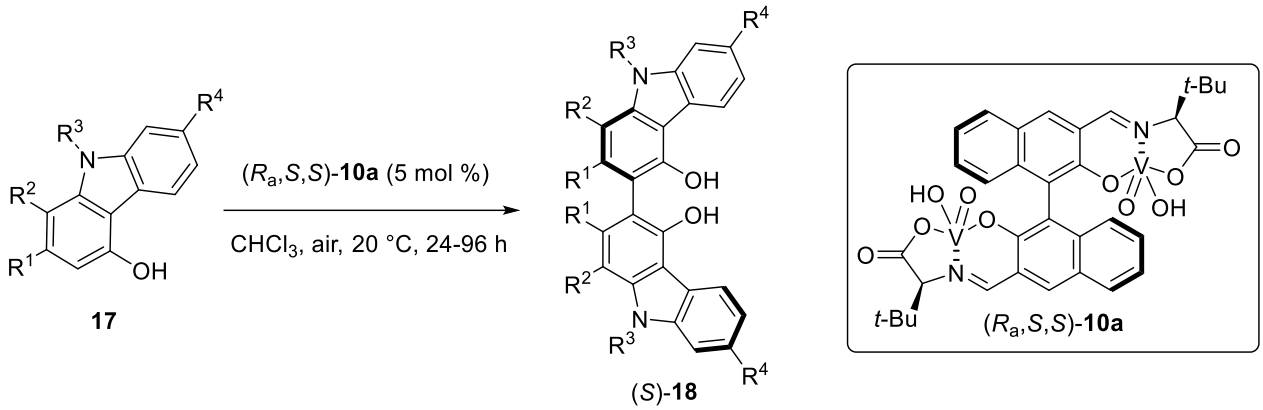

A test tube was charged with 4-hydroxycarbazole **17** (1.0 equiv), dinuclear vanadium catalyst (R_a,*S*,*S*)-**10a** (5 mol%), and $CHCl_3$ (0.1 M) under air at room temperature. The mixture was stirred for 24 h, at 20°C. The reaction mixture was then filtered through a short pad of silica gel and the solvent was evaporated. The crude product was purified by silica gel column chromatography to afford homo-coupling product **18**.

(*S*)-2,2',9,9'-Tetramethyl-*9H*,*9'H*-[3,3'-bicarbazole]-4,4'-diol (18a)

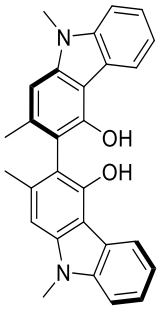

^{1}H NMR (400 MHz, $CDCl_3$): δ 8.28 (d, *J* = 7.8 Hz, 2H), 7.47 (ddd, *J* = 7.8, 7.3, 0.9 Hz, 2H), 7.41 (d, *J* = 8.2 Hz, 2H), 7.26 (ddd, *J* = 7.6, 7.3, 1.1 Hz, 2H), 7.05 (s, 2H), 5.48 (s, 2H), 3.89 (s, 6H), 2.21 (s, 6H).

^{13}C NMR (100 MHz, $CDCl_3$): δ 150.80, 143.29, 140.65, 137.45, 124.88, 122.88, 122.24, 119.57, 109.06, 109.04, 108.09, 102.70, 29.42, 20.98.

HRMS (ESI): calcd for $C_{28}H_{25}N_2O_2$: *m/z* 421.1911 $[M + H]^+$, found 421.1912.

IR (KBr): 3505, 2923, 2853, 1636, 1605, 1462, 1414, 1257, 814, 746 cm^{-1}.

mp: 260-262 °C.

Enantiomeric ratio: 95.1:4.9, determined by HPLC (Chiral Pak IbN-5, hexane/2-propanol = 99/1; flow rate 1.0 mL/min; 25 °C; 240 nm) first peak: t_R = 55.2 min, second peak: t_R = 68.9 min.

$[\alpha]_D^{24}$ 283.2 (*c* 0.11, $CHCl_3$) for 95.1:4.9 er.

(*S*)-1,1',2,2'-Tetramethyl-*9H*,*9'H*-[3,3'-bicarbazole]-4,4'-diol (18b)

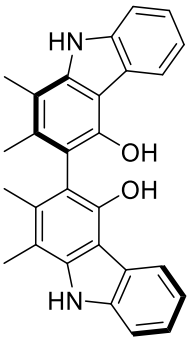

^{1}H NMR (400 MHz, ($CDCl_3$): δ 8.17 (d, *J* = 7.6 Hz, 2H), 7.92 (brs, 2H), **7.39 (d, *J* = 7.6 Hz, 2H), 7.31 (t, *J* = 7.4 Hz, 2H), 7.16 (t, *J* = 7.4 Hz, 2H),** 5.23 (brs, 2H), 2.40 (s, 6H), 2.01 (s, 6H).

^{13}C NMR (100 MHz, ($CDCl_3$): δ 148.4, 141.0, 138.9, 134.6, 124.8, 123.2, 122.9, 119.9, 110.6, 110.4, 110.0, 109.2, 16.7, 13.6.

HRMS (ESI): calcd for $C_{28}H_{24}N_2O_2$: *m/z* 443.1730 [M + Na]+, found 443.1725.

IR (KBr): 3500, 3432, 3055, 2923, 1635, 1612, 1448, 1413, 1385, 1329, 1240, 1212, 1140, 1112, 1038, 750 cm^{-1}.

mp: 252-254 °C.

Enantiomeric ratio: 89.8:10.2, determined by HPLC (Chiralpak IA, hexane/2-propanol = 4/1; flow rate 1.0 mL/min; 25 °C; 335 nm) first peak: t_R = 13.0 min, second peak: t_R = 23.7 min. $[\alpha]_D^{14}$ +189.2 (*c* 2.93, $CHCl_3$) for 89.8:10.2 er.

2.9 References:

28. Aikawa K.; Miyazaki Y.; Mikami K. *Bull. Chem. Soc. Jpn.* **2012**, *85*, 201-208.
29. (a) Cadogan, J.; Cameron-Wood, G.M.; Mackie, R. K.; Searle, R. J. G. *J. Chem. Soc*. **1965**, 4831-4837. (b) Appukkuttan, P.; Van der Eycken.; Dehaen, W. *Synlett*, **2005**, *1*, 127-133.
30. Takizawa, S.; Katayama, T.; Sasai, H. *Chem Commun.* **2008**, 4113-4122.
31. Decomposition of **17a** was observed when the reaction was conducted under an O_2 atmosphere.
32. Sako, M.; Aoki, T.; Zumbrägel, N.; Schober, L.; Gröger, H.; Takizawa, S.; Sasai, H. *J. Org. Chem.* **2019**, *84*, 1580
33. M. Oki, *Top. Stereochem*., **1983**, *14*, 1
34. a) Hoen, R.; Leleu, S.; Botman, P. N. M.; Appelman, V. A. M.; Feringa, B. L.; Hiemstra, H.; Minnaard, A. J.; van Maarseveen, J. H. *Org. Biomol. Chem.*, **2006**, *4*, 613. b).Botman,

P. N. M.; Amore, A.; van Heerbeek, R.; Back, J. W.; Hiemstra, H.; Reek, J. N. H.; van Maarseveen, J.H. *Tetrahedron Lett.*, **2004**, *45*, 5999.

35. Botman, P. N. M.; Fraanje, J.; Goubitz, K.; Peschar, R.; Verhoeven, J. W.; van Maarseveen J. H.; Hiemstra H. *Adv. Synth. Catal*., **2004**, *346*, 743.
36. Feature article for the dual activation: Sasai, H.; Takizawa, S. *Chem. Commun.* **2008**, 411331
37. Sako M.; Ichinose K.; Takizawa S.; Sasai, H. *Chem. Asian J.* **2017**, *12*, 1305.
38. Sako, M.; Takeuchi, Y.; Tsujihara, T.; Kodera, J.; Kawano, T.; Takizawa, S.; Sasai, H. *J. Am. Chem. Soc*. **2016**, *138*, 11481–11484.

Chapter 3

3. Enantioselective Hetero-Coupling of Hydroxycarbazole.

In contrast to homo coupling reactions, hetero-coupling occurs when two different reaction substrates bind to each other. The development of a highly enantio- and regio-selective hetero-coupling while avoiding the formation of by-products is a challenging task. This chapter will be focused on the hetero-coupling of 3-hydroxycarbazole and 2-naphthol to obtain convenient access to hetero-coupled products with high yield and optical purity.

3.1 Reaction Mechanism of Hetero-coupling of Hydroxycarbazoles

Pappo[8o] hypothesized that the steric and/or electronic factors of the coupling partner, such as the ability of the binding to the metal catalyst, oxidation potential, and nucleophilicity, are crucial considerations for the requirement of a cross-selective coupling. The reaction involves the coupling between an electrophilic radical and an anionic acceptor. This cross-coupling is favoured when there is a sufficient difference in the redox potentials ($E \geq 0.25$ V) of the two coupling partners to ensure selectivity in phenolic oxidative coupling cross-coupling reactions.

Accordingly, we measured oxidation potential by cyclic voltammetry (CV) method 3-hydroxy carbazole (shown in red) and 2-naphthol (shown in blue) (**Diagram A**). As a result, cyclic voltammetry as shown below and it was found the oxidation potential of 3-hydroxycarbazole was $E_{(OX)} = 0.71$ eV, and that 2-naphthol was $E_{(OX)} = 1.271$ eV. From the above outcomes, it was confirmed that 3-hydroxycarbazole has a lower oxidation potential than 2-naphthol. 3-hydroxycarbazole is easily oxidized with vanadium metal and higher oxidation potential suggests higher nucleophilicity of 2-naphthol. These results suggest cross-coupling, which is the basic requirement to maintain reactivity between two substrates to develop a successful hetero-coupling reaction.

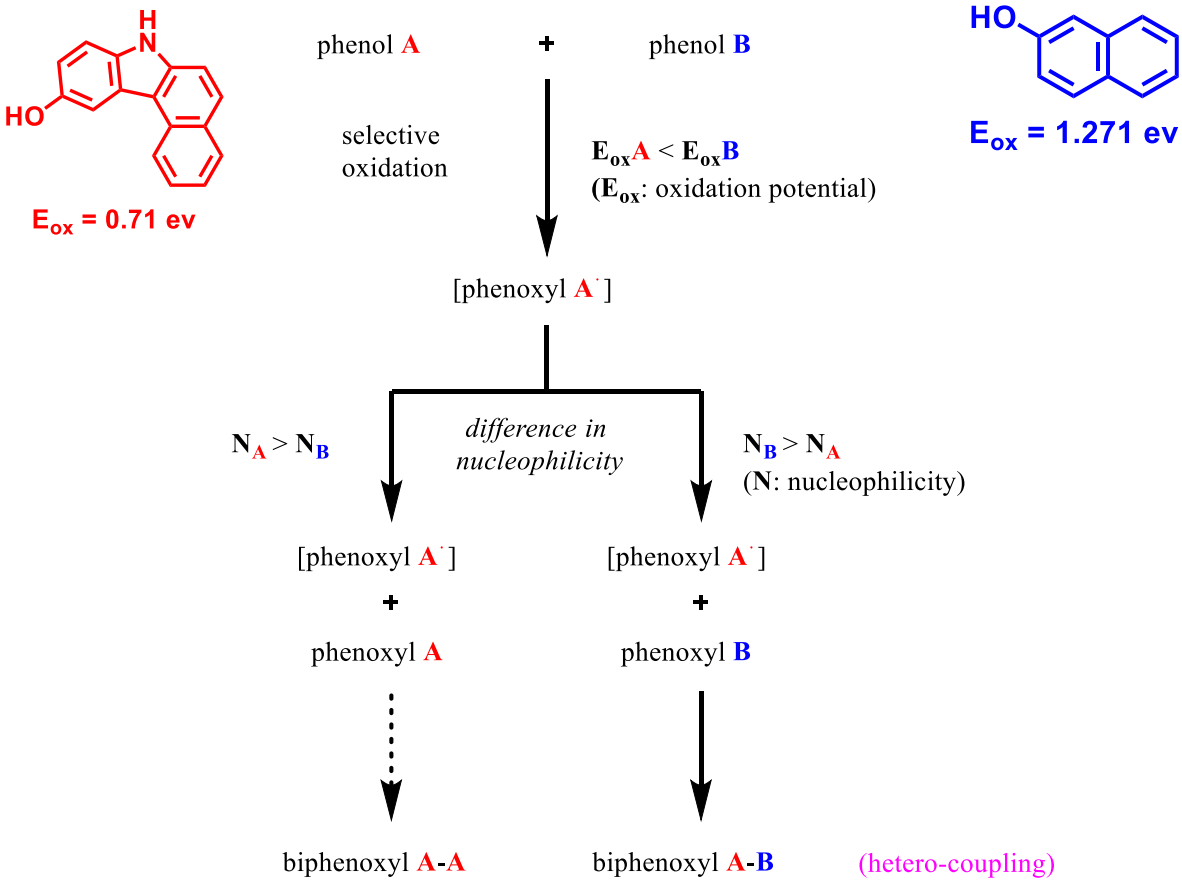

Diagram A. Development of efficient oxidative hetero couplings

3.2 Screening of Vanadium Catalyst and Optimization of Condition:

In the initial development, the difference in catalytic activity between the mononuclear vanadium complex and the dinuclear vanadium complex in this reaction was verified (**Table 4.1**). The optimization of reaction conditions was carried out with 3-hydroxycarbazole (**9a**) and 2-naphthol (**1a**) as model substrates in a 1:1 ratio in the presence of air at 30 °C. The catalyst loading was maintained with 5 mol% and 10 mol% of dinuclear vanadium complex (R_a,*S*,*S*)-**10a** and mononuclear vanadium complex (R_a, *S*)-**8b**, respectively. The dinuclear vanadium complex (R_a,*S*,*S*)-**10a** afforded the Major hetero-coupling product **20a** in 73% yield and 42% ee along with the Minor homo-coupling **2aa** in 10% yield. On the other hand, the mononuclear vanadium complex (R_a,*S*)-**8b** resulted in an increased yield (81%) of the hetero-coupling product **20a** by suppressing the homo-coupling product **2aa** with less than 5% yield.

The rationale behind the increased formation of **2aa** while using (R_a,*S*,*S*)-**10a** is considered to be the reaction-promoting effect due to the dual activation mechanism of (R_a,*S*,*S*)-**10a**. These results encouraged us to explore the mononuclear vanadium catalyst for the development of hetero-coupling reactions with different substrates.

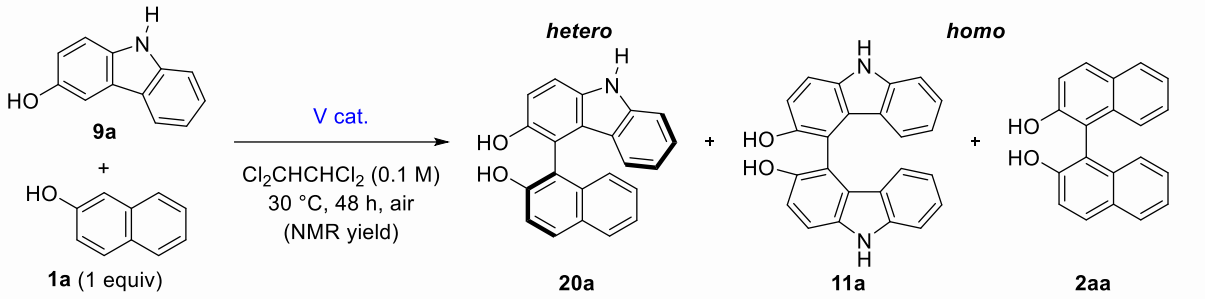

	20a	11a	2aa
dinuclear V catalyst (R_a,*S*,*S*)-**10a** (5 mol%)	73% yield 42% ee	—	10% yield
mononuclear V catalyst (R_a,*S*)-**8b** (10 mol%)	81% yield 37% ee	—	>5% yield

Table 4.1 Initial screening of chiral vanadium catalyst for hetero coupling

As mononuclear vanadium catalyst showed good reactivity to generate hetero-coupled product **20a**, further optimization of reaction conditions using mono nuclear vanadium catalyst (R_a,*S*)-**8b** was carried out.

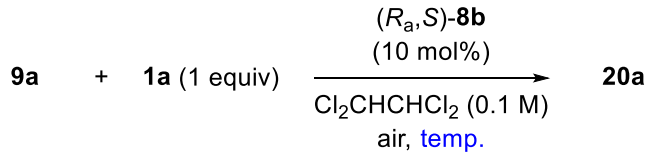

entry	temp. (°C)	time (h)	NMR yield (%)	ee (%)
1	10	48	53	40
2	20	48	69	40
3	30	48	81	37
4	40	48	91	32
5	50	24	90	21

Table 4.2 Temperature screening for hetero-coupling

Using a mononuclear vanadium complex (R_a,S)-**8b**, the reaction temperature (10~50 °C) was screened (**Table 4.2**). It was observed that the lower reaction temperature (10 °C and 20 °C),

afforded **20a** with 40 % ee and lower yields along with longer reaction time (entries 1, 2). A slight increase in the temperature (40 °C and 50 °C) was able to improve the yield but the enantioselectivity was reduced (entries 4, 5). The reaction at 30 °C for 48 hours resulted in acceptable yield and enantioselectivity for further exploration.

Subsequently, the structural modifications were investigated with mononuclear vanadium catalyst to find the best suitable catalyst for the hetero-coupling reaction as shown in **(Table 4.3)**. It was observed that the substitution at the 3'-position of (R_a,S)-**8** is useful to improve the yield and enantioselectivity of **20a**. Instead of (R_a,*S*)-**8b**, the diastereomeric vanadium catalyst (S_a,*S*)-**8b** resulted in 75% yield and 22% ee. The decreased enantioselectivity could arise due to the *mismatched pair* in (S_a,*S*)-**8b**. The replacement of the *t*-butyl group on vanadium catalyst by the *iso*-propyl group (R_a, *S*)-**21** afforded 95% yield but low enantioselectivity of 30%.

Further substitution at the 3'-position, was carried out with bulky substrates to evaluate the impact on the enantioselectivity. Substitution of the phenyl group at position 3' (R_a,*S*)-**22** showed a good yield but a low 47% ee; whereas the comparable (R_a,*S*)-**23** gave 95% yield and 56% ee. Together with this small methyl group substitution at position 3' (R_a,*S*)-**24** achieved 49 % ee. With the halogen group installed at position 3' (R_a,*S*)-**25**, the result showed an acceptable yield but low ee 44%.

Upon replacing 3,5-bis(trifluoromethyl) benzene at position 3' (R_a,*S*)-**26**, the enantioselectivity dropped drastically by 9% owing to the electron-withdrawing nature of the trifluoro group. A naphthalene bulky group at position 3' to create steric hindrance (R_a,*S*)-**27** 82% yield and 42% enantioselectivity were obtained with continued efforts, 3,5-dimethyl phenyl at 3' position (R_a,*S*)-**28** and 3,5-di-*iso*propyl phenyl (R_a,*S*)-**29** showed reasonable yield and moderate enantioselectivity of up to 45 %. Finally, the 2,6-dimethyl phenyl substitution on phenyl (R_a,*S*)-**30** showed a good yield of 92% and good enantioselectivity of 63%. Subsequently, the screening of the solvents was performed using (R_a,*S*)-**30** mono nuclear vanadium catalyst at 30 °C in the presence of air as shown in (**Table 4.4).**

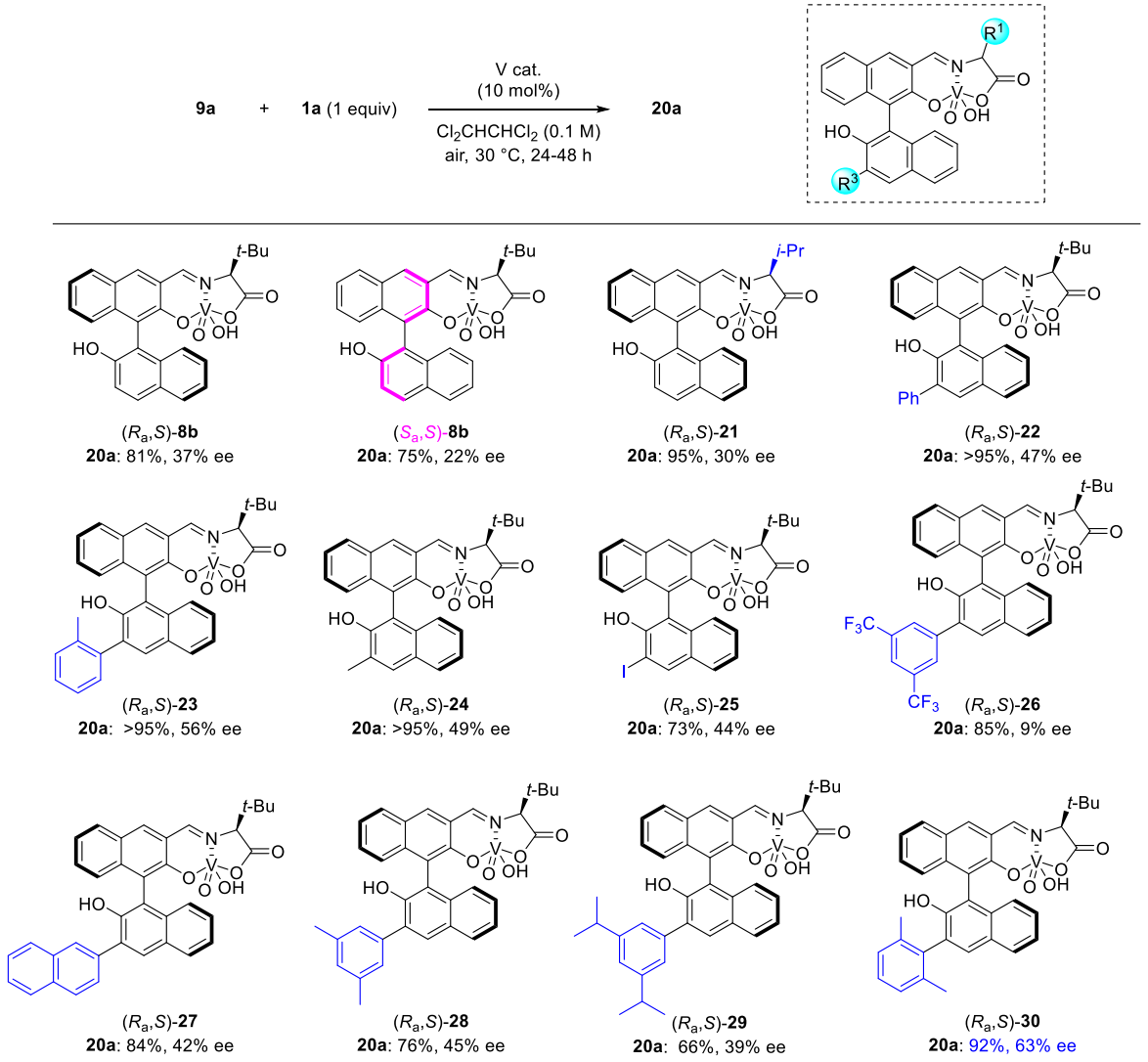

Table 4.3 Screening of mono nuclear vanadium catalyst

It was found that the chlorine-based organic solvents (entries 1–7) are convenient to afford **20a** in high yield (92 %, > 95 %). On the contrary, the hydrocarbon-based solvents were not suitable due to decreased yield and enantioselectivity (entries 8–12). Similarly, the cyclic ethereal solvents were also found not suitable (entries 13–16) with low reaction rates and yields. Extending the reaction time from 48 to 96 h using 1,4-dioxane as the solvent delivered the highest enantioselectivity and improved yield of **20a** in 74 % and 81 % ee (entry 17).

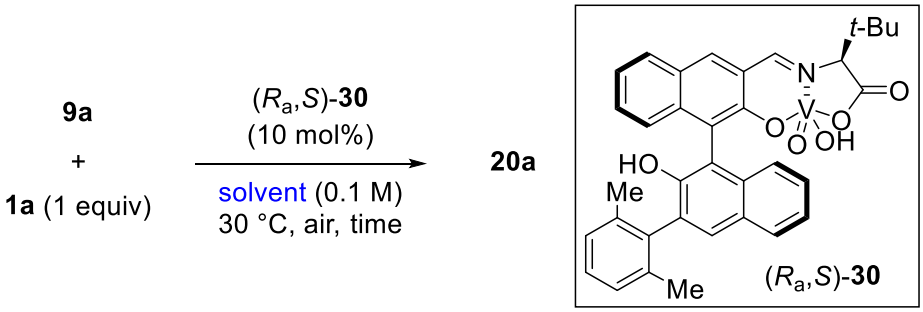

entry	solvent	time (h)	NMR yield (%)	ee (%)
1	CH_2Cl_2	24	92	61
2	$CHCl_3$	24	69	60
3	CCl_4	24	57	56
4	$ClCH_2CH_2Cl$	24	78	61
5	$Cl_2CHCHCl_2$	24	>95	63
6	$Cl_2C=CCl_2$	24	67	60
7	PhCl	24	81	59
8	toluene	24	79	57
9	*o*-xylene	24	77	58
10	*m*-xylene	24	72	58
11	*p*-xylene	24	79	61
12	mesitylene	24	79	59
13	THF	48	20	76
14	2-MeTHF	48	59	71
15	MTHP	48	59	70
16	1,4-dioxane	48	40	83
17	1,4-dioxane	96	74	81

Table 4.4 Solvent Screening

In 2017, Kozlowski *et al*. reported that the addition of acetic acid and lithium chloride was effective in improving the product yield and enantioselectivity in oxidative homo-coupling reactions of phenol and hydroxycarbazole using vanadium catalysts.[18b] Therefore, the additives were examined (**Table 4.5**). Since the yield of **20a** was slightly improved when 1.0 equivalent of acetic acid was added (entry 2), the amount of acetic acid added was further increased (entries 3-5). As a result, although the yield was improved, **20a** was obtained with low enantioselectivity (51% ee). The addition of 0.5 equivalents of lithium chloride improved the yield of **20a** and the enantioselectivity, providing 85% and 86% ee, respectively (entry 10). Increased lithium chloride addition slightly improved the enantioselectivity of **20a** but reduced

the yield (entries 11-16). The reason for the decrease in the yield could be that the mixing efficiency has deteriorated due to a large addition amount. Other additives were also considered, but no significant effects were observed (entries 8, 9, 17, 18). From the above results, the lithium chloride 3.0 equivalent, which gives good results in terms of yield and enantioselectivity, was determined as the optimal condition (entry 14).

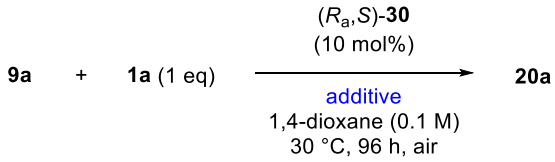

entry	additive (equiv)	NMR yield (%)	ee (%)	entry	additive (equiv)	NMR yield (%)	ee (%)
1	none	74	81	10	LiCl (0.5)	85	86
2	AcOH (1.0)	77	81	11	LiCl (1.0)	84	85
3	AcOH (2.0)	70	73	12	LiCl (2.0)	84	86
4	AcOH (5.0)	74	62	13	LiCl (2.5)	83	86
5	AcOH (10.0)	83	51	14	LiCl (3.0)	85	88
6	PhCOOH (0.5)	85	80	15	LiCl (5.0)	84	88
7	TMSCl (0.5)	20	15	16	LiCl (10.0)	78	88
8	NH_4Cl (3.0)	75	82	17	$LiClO_4$ (1.0)	77	74
9	LiBr (1.0)	82	81	18	$Mg(ClO_4)_2$ (1.0)	63	75

Table 4.5 Screening of additives

The impact of the concentration of the reaction solvent on the reactivity of 3-hydroxycarbazole (**9a**) was examined as shown in (**Table 4.6**). When the reaction was carried out with 0.05 M concentration, a little change in the enantioselectivity was observed with a reduced yield to 61 % (entry 1). The increase in the concentration improved the yield to 80 % but the enantioselectivity was reduced to 73 % (entry 3). From the above results, 0.1 M, which gives good results for yield and enantioselectivity, was determined as the optimal concentration of the reaction solvent (entry 2).

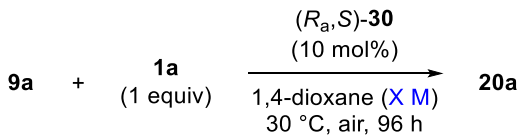

entry	concentration (M)	NMR yield (%)	ee (%)
1	0.05	61	82
2	0.1	74	81
3	0.2	80	73

Table 4.6 Concentration effect

3.3 Substrate Scope:

After successfully optimizing the reaction conditions for the hetero-coupling of 3-hydroxycarbazole (**9**) with 2-naphthol (**1**), the substrate scope and limitations were investigated as shown in (**Scheme 9a**).

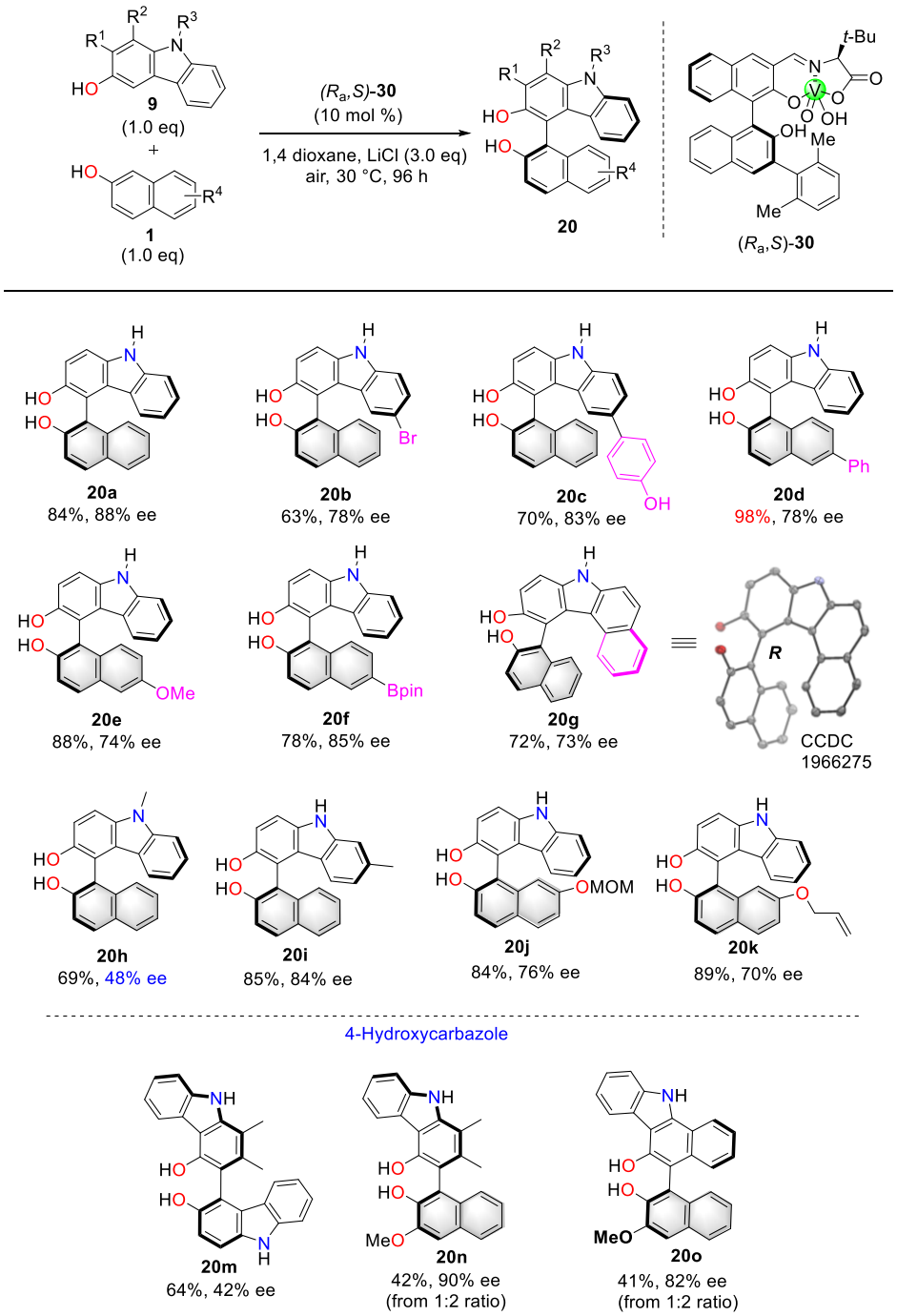

Scheme 9a. The substrate scope

The Bromo substituted carbazole **9b** affords **20b** in 63 % yield and 78 % ee. Especially, this derivative could be interesting from the ligand development of view. Similarly, the extended phenol ring on the carbazole moiety **9c** also affords **20c** in 70 % yield and 83 % ee.

Subsequently, the substitution of 2-naphthols such as phenyl (**1dd**), methoxy group (**1ee**), and (pinacolato)boron (**1ff**), showed good reactivity and afforded the corresponding products **20d-20f** (78-94 % yield) and (74-85 % ee). The axially chiral compound **20f** can be used as a precursor of the Suzuki-Miyaura coupling reaction.

The extended hydroxycarbazole, *7H*-benzo[*c*]carbazol-10-ol (**9g**), produced the coupled product **20g** in 72% yield with 73% ee. The absolute configuration of **20g** was determined to be *R* by X-ray crystallographic analysis. After nitrogen encapsulation with a methyl group of 3-hydroxycarbazole (**9h**), **20h** gave the corresponding product in 69 % yield and 48 % ee. The 2-position methyl substituent 3-hydroxycarbazole (**9i**) and 7-position substitution on 2-naphthol **1jj** and **1kk** furnished the corresponding products **20j** and **20k** in 84–89 % yield and 70–76 % ee, respectively. 4-Hydroxycarbazole (**17b**) and 3-hydroxycarbazole (**9a**) were also found to be suitable substrates for the hetero-coupling with the 2-naphthol derivative (**1nn**), affording C_1-symmetric biaryl **20m**, **20n**, and **20o**, respectively, with up to 90% ee.

3.4 Control Experiment:

Control experiments were performed to obtain further insight into the reaction mechanism. As a result of adding the radical scavenger TEMPO under optimal conditions, the product yield was reduced to 20% (**Scheme 10-A**). The presence of radical intermediates has been suggested. Further, 2-naphthol **1ee** with methoxy group and 2-naphthol **1ii** with Bromo group were used simultaneously in the reaction to examine the ratio of the coupling product (**Scheme 10-B**).

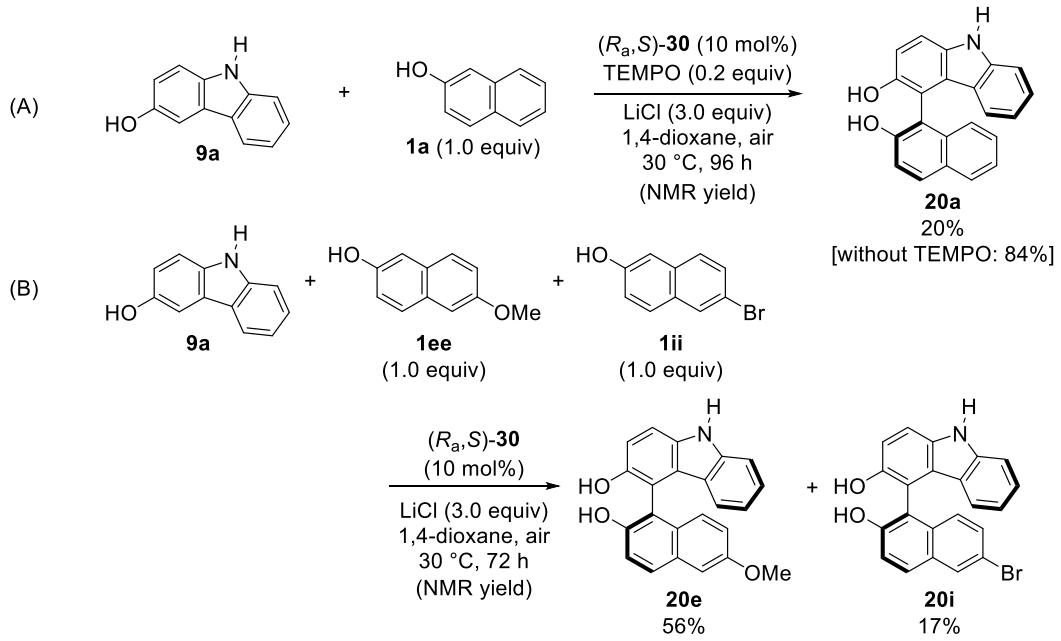

Scheme 10. Control experiment

Generally, when the reaction proceeds under radical-radical coupling, a homo-coupling product having a low oxidation potential and being easily oxidized can be obtained in large amounts. On the other hand, in the case of radical-anionic coupling **1ee** having a higher nucleophilicity value than **1ii**, the radical cation of **9a** preferentially attacks, and a large amount of hetero-coupling product **20a** should be obtained. As a result of the actual experiment, hetero-coupling products were obtained at a rate of **20e:20i** = 56%:17%, and homo-coupling products were not observed. The above results suggest that this reaction undergoes a radical anionic coupling reaction mechanism.

3.5 Proposed Reaction Mechanism:

A plausible catalytic cycle for the oxidative hetero-coupling of hydroxycarbazoles **9** with 2-naphthols **1** is illustrated in **(Scheme 11**). The condensation of the mononuclear vanadium(V) complex (R_a,*S*)-**30** with **9a** generates intermediate **A**. Along with involving activation of the vanadium complex by LiCl coordination of Li+ on the vanadium oxy group generates a more Lewis acidic species and also avoids oligomerization of vanadium catalyst.[18b]

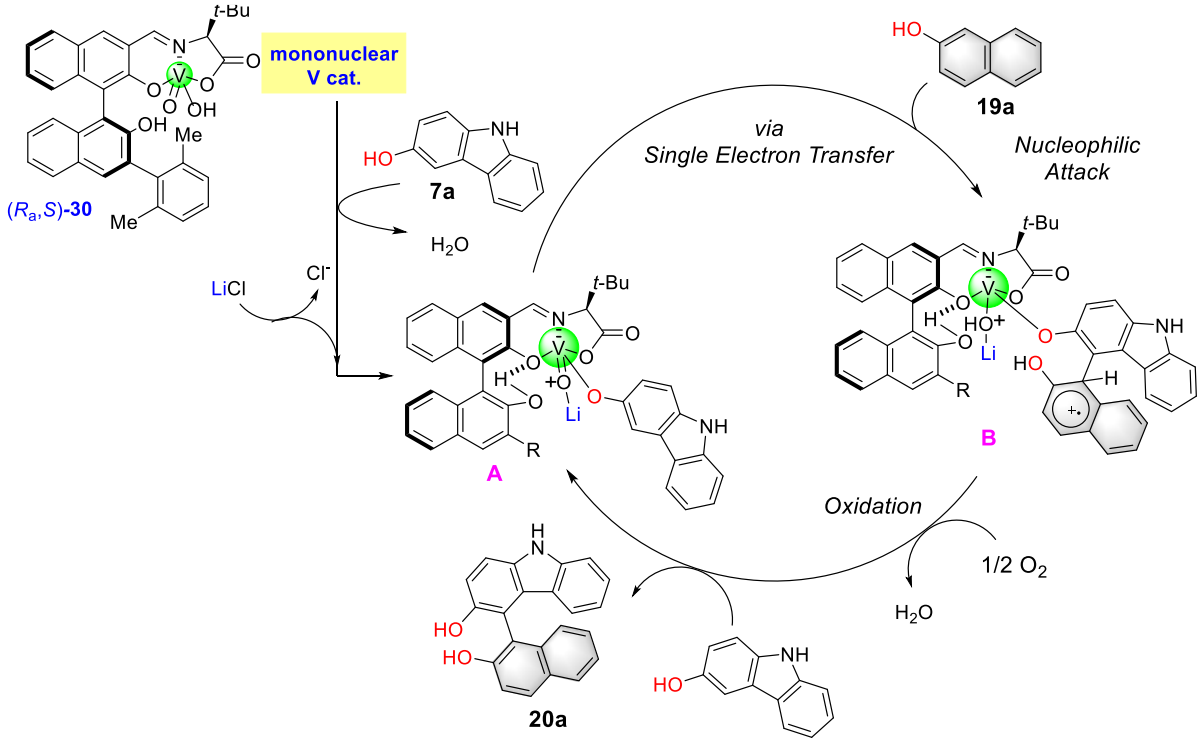

Scheme 11. Plausible reaction mechanism for the oxidative hetero-coupling of 3-hydroxycarbazoles **9** with 2-naphthols **1**

Subsequently, intermediate **A** undergoes a single electron transfer (SET) from the carbazole moiety to vanadium(V) to generate the conceivable electrophilic radical intermediate **B**, since **9a** is more easily oxidized than **1a**. (**Diagram A**) This is followed by an intermolecular radical–anion coupling to afford intermediate **B** with the formation of a new carbon-carbon bond through the nucleophilic attack of 2-naphthols. Re-oxidation of vanadium (IV) to vanadium(V) by molecular oxygen proceeds in the air to give intermediate **A**. After vanadium(V) complex (R_a,*S*)-**30**. With a 1: 1 molar ratio of the two starting materials, this catalytic system successfully and efficiently produced hetero-coupling products **20a** with up to 98% yield and 90% ee. To confirm the mechanism, further applications of hetero-coupling reaction switched the nucleophile from 2-naphthol to β-ketoester will be discussed in **Chapter 4**.

The following **Figure 4a** shows the estimated expression mechanism of stereoselectivity in the reaction. Once the hydroxycarbazole is electron-oxidized by vanadium, a nucleophilic attack of the 2-naphthol substrate occurs to avoid steric repulsion with the 2,6-dimethyl phenyl group at the 3′ positions on the binaphthyl backbone of the catalyst, resulting in preferential *R*-form products. We have developed a highly enantioselective and catalytic oxidative hetero-coupling of 3-hydroxycarbazoles **9** with 2-naphthols **1** using a newly developed mononuclear vanadium(V) complex (R_a,*S*)-**30**. With a 1: 1 molar ratio of the two starting materials, this catalytic system successfully and efficiently produced hetero-coupling products **20** with up to 98% yield and 90 % ee.

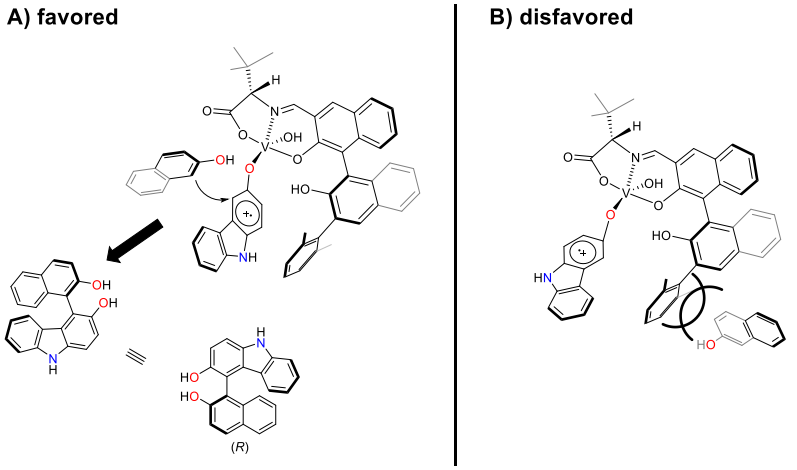

Figure 4. Estimated expression mechanism of stereoselectivity

3.6 ^{51}V-NMR chart of the mononuclear vanadium catalyst

^{51}Vanadium NMR experiment was carried out in 1,4-dioxane and detected two peaks in the NMR chart as shown in (**Figure 4b).** It unequivocally supports the occurrence of the mixture of monomer and dimer of vanadium catalyst in the catalytic reaction.

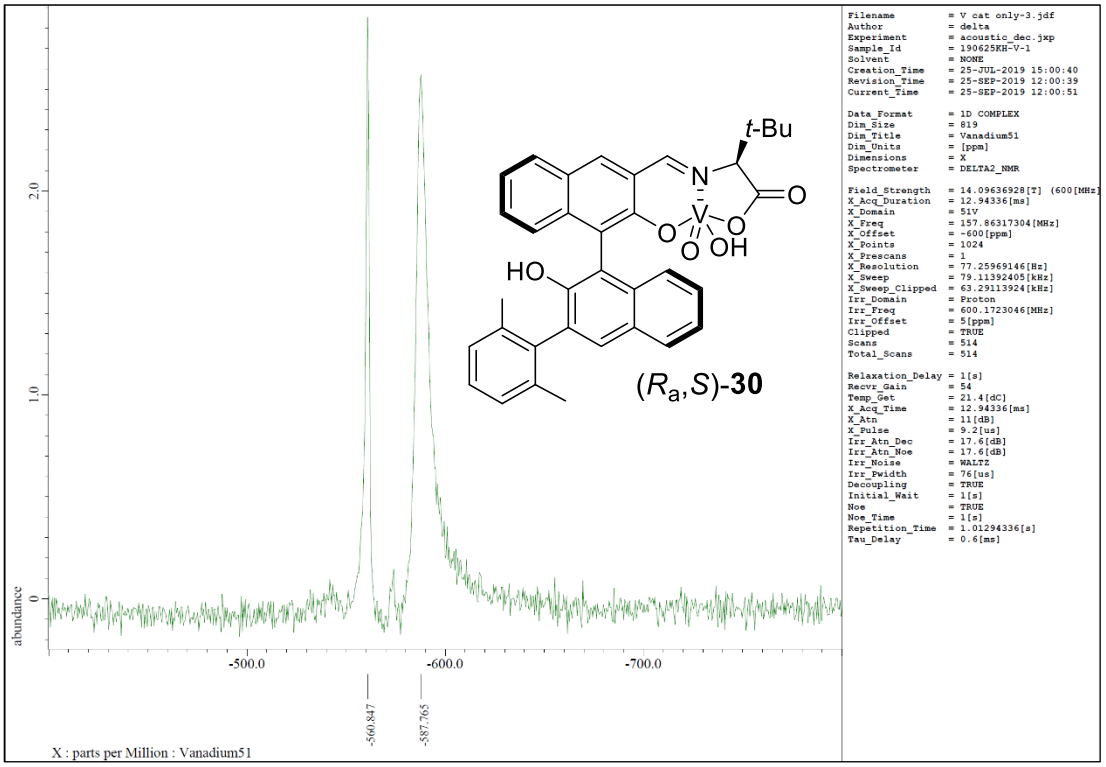

Figure 4b. ^{51}V-NMR chart of V cat. (R_a,*S*)-**30** in 1,4-dioxane at room temperature.

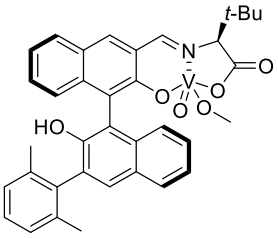

HRMS (ESI): calcd for $C_{36}H_{34}NNaO_6V$: *m*/*z* 650.1723 [M + Na]$^+$, found 650.1724.

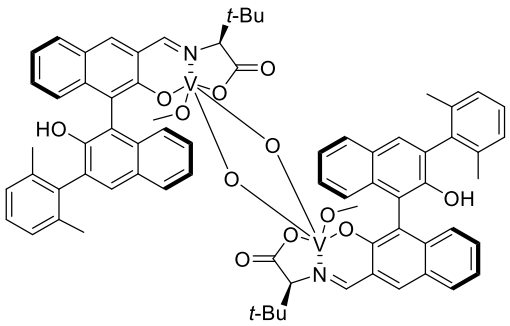

HRMS (ESI): calcd for $C_{72}H_{68}N_2NaO_{12}V_2$: *m*/*z* 1277.3549 [M + Na]$^+$, found 1277.3560.

Also, HRMS observed the mass of monomer and dimer species. The dimer species have low asymmetric induction as well as a lower catalytic activity than that monomer. A mechanistic study (**Scheme 11 Intermediate A**) supports the role of additive LiCl which is responsible for enhancing the activity of catalyst as well as avoiding the formation of dimer species of vanadium catalyst.

3.7 Experimental section:

Preparation of mononuclear vanadium complexes

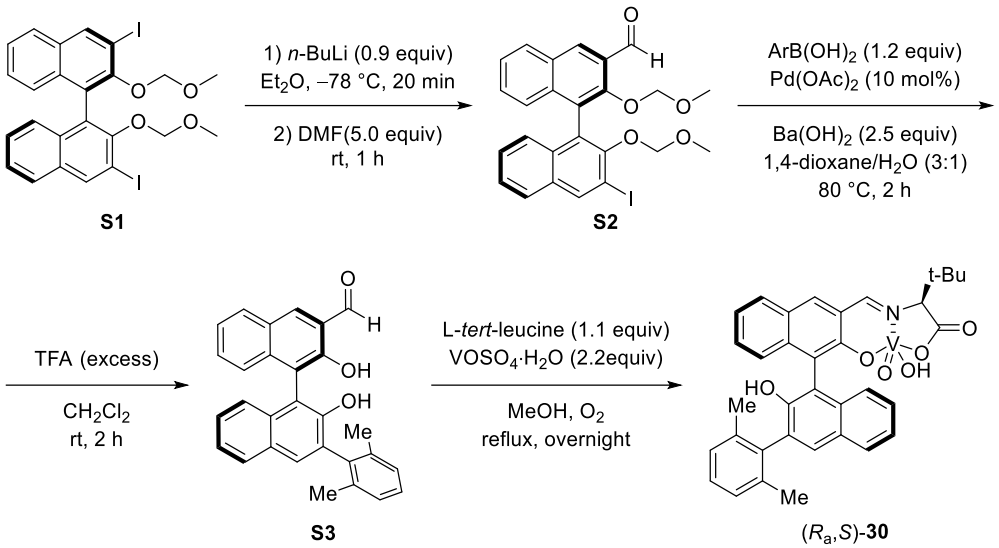

(*R*)-3'-(2,6-dimethylphenyl)-2,2'-dihydroxy-[1,1'-binaphthalene]-3-carbaldehyde (**S3**)

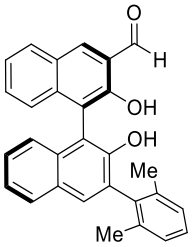

The compound **S3** was prepared according to the literature procedure.[38] A suspension of **S2** (250.0 mg, 0.47 mmol), (2,6-dimethyl phenyl) boronic acid (78.1 mg, 0.52 mmol), $Pd(PPh_3)_4$ (54.7 mg, 0.047 mmol) and $Ba(OH)_2$ (202.7 mg, 1.18 mmol) in degassed water/1,4-dioxane (1/3, 4.7 mL) was stirred for 3 h at 80 °C. After cooling, the reaction mixture was then filtered through a short pad of silica gel and the solvent was evaporated. The crude product was purified by silica column chromatography to give a coupling product. Subsequent deprotection of the methoxymethyl group was performed. Trifluoroacetic acid (excess) was dded to a solution of coupling product in CH_2Cl_2 (4.7 mL) at room temperature. The mixture was stirred for 2 h. After concentrated, the reaction mixture was purified by silica column chromatography to afford (*R*)-3'-(2,6-dimethyl phenyl)-2,2'-dihydroxy-[1,1'-binaphthalene]-3-carbaldehyde (**S3**) in 77% yield in 2 steps as a yellow solid.

^{1}H NMR (400 MHz, $CDCl_3$): δ 10.54 (s, 1H), 10.20 (s, 1H), 8.35 (s, 1H), 8.02-7.99 (m, 1H), 7.87 (d, J = 7.8 Hz, 1H), 7.74 (s, 1H), 7.47-7.17 (m, 10H), 4.41 (s, 1H), 2.18 (s, 6H).

^{13}C NMR (100 MHz, $CDCl_3$): δ 196.6, 154.0, 149.0, 138.5, 137.9, 137.7, 137.4, 135.4, 133.3, 130.8, 130.0, 129.7, 129.2, 129.1, 128.3, 128.2, 127.8, 127.7, 126.5, 125.0, 124.5, 123.6, 122.1, 116.8, 113.9, 20.6.

HRMS (APCI): calcd for $C_{29}H_{23}O_3$: *m/z* 419.1647 $[M + H]^+$, found 419.1632.

$[\alpha]_D^{26}$ +50.93 (*c* 0.30, $CHCl_3$).

Mononuclear vanadium complex (R_a,*S*)-30

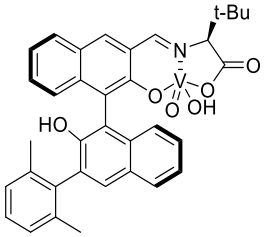

A round-bottomed flask was charged with **S3**(152.2 mg, 0.36 mmol), L-*tert*-leucine (52.5 mg, 0.40 mmol), $VOSO_4$•xH_2O (144.8 mg, 0.80 mmol), MS 3A (360 mg), MeOH (9.1 mL) under O_2 (balloon). The reaction mixture was refluxed, and the consumption of 14 was monitored by TLC. The resulting solution was gradually cooled down to r.t. and filtered through Celite to remove MS 3A. The filtrate was evaporated, and the resulting black solid was dissolved in CH_2Cl_2 and washed with H_2O. The organic phase was dried over anhydrous Na_2SO_4 and concentrated in a vacuum to give desired vanadium complex (R_a,*S*)-**30** in 73% yield as a dark green solid.

^{1}H NMR (400 MHz, CD_3OD): δ 8.90 (s, 1H), 8.43 (s, 1H), 7.97 (s, 1H), 7.80-7.78 (m, 1H), 7.59-7.58 (m, 1H), 7.32-7.10 (m, 9H), 4.22 (s, 1H), 2.12 (s, 6H), 1.22 (s, 9H).

^{13}C NMR (100 MHz, CD_3OD): δ 180.6, 169.2, 151.9, 140.2, 139.7, 139.3, 139.24, 139.18, 139.0, 136.0, 132.4, 131.7, 131.5, 131.4, 130.6, 129.8, 129.4, 129.2, 127.97, 127.95, 127.3, 127.0, 126.1, 125.2, 118.9, 118.4, 85.0, 39.4, 29.1, 21.9.

HRMS (ESI): calcd for $C_{36}H_{34}NNaO_6V$: *m/z* 650.1723 $[M + OMe – OH + Na]^+$, found 650.1710.

Enantioselective oxidative hetero-coupling of 3-hydroxycarbazole and 2-naphthol catalyzed by vanadium(V) Complex

A test tube was charged with 3-hydroxycarbazole (1.0 eq), 2-naphthol (1.0 eq), mononuclear vanadium catalyst (10 mol%), lithium chloride (3.0 eq) and 1,4-dioxane (0.1 M) under air at 30 ℃. The mixture was stirred for 96 h. The reaction mixture was then filtered through a short

pad of silica gel and the solvent was evaporated. The crude product was purified by silica gel column chromatography to afford the hetero-coupling product.

4-(2-hydroxynaphthalen-1-yl)-9*H*-carbazol-3-ol (20a)

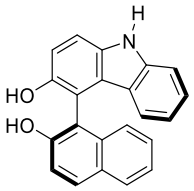

^{1}H NMR (400 MHz, $CDCl_3$): δ 8.12 (s, 1H), 8.03 (d, J = 8.7 Hz, 1H), 7.93 (d, J = 8.2 Hz, 1H), 7.53 (d, J = 8.7 Hz, 1H), 7.44-7.25 (m, 7H), 6.77 (t, J = 7.3 Hz, 1H), 6.66 (d, J = 7.8 Hz, 1H), 5.26 (s, 1H), 4.72 (s, 1H).

^{13}C NMR (100 MHz, $CDCl_3$): δ 152.3, 148.2, 140.4, 134.6, 132.8, 131.3, 129.4, 128.4, 127.5, 126.0, 124.1, 124.0, 122.6, 122.4, 121.4, 119.3, 117.8, 115.0, 112.6, 111.8, 110.7, 110.5.

HRMS (APCI): calcd for $C_{22}H_{16}NO_2$: *m/z* 326.1181 $[M + H]^+$, found 326.1176.

IR (KBr): 3409, 3059, 2926, 1620, 1499, 1442, 1276, 1168, 1147, 898, 817, 748 cm^{-1}.

mp: 113-115 °C. White solid.

Enantiomeric excess: 88%, determined by HPLC (Chiralpak IA, hexane/2-popanol = 4/1; flow rate 1.0 mL/min; 25 °C; 220 nm) first peak: t_R = 16.8 min, second peak: t_R = 20.4 min. $[\alpha]_D^{20}$ –82.90 (*c* 0.18, $CHCl_3$) for 88% ee.

4-(2-hydroxynaphthalen-1-yl)-7-methyl-9*H*-carbazol-3-ol (20i)

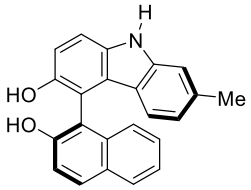

^{1}H NMR (400 MHz, $CDCl_3$): δ 8.02 (d, J = 9.2 Hz, 1H), 7.99 (s, 1H), 7.92 (d, J = 8.2 Hz, 1H), 7.49 (d, J = 8.7 Hz, 1H), 7.42 (d, J = 8.7 Hz, 1H), 7.39-7.23 (m, 4H), 7.17 (s, 1H), 6.59 (dd, J = 8.2, 0.9 Hz, 1H), 6.52 (d, J = 8.2 Hz, 1H), 5.25 (s, 1H), 4.68 (s, 1H), 2.38 (s, 3H)

^{13}C NMR (100 MHz, $CDCl_3$): δ 152.3, 148.2, 140.9, 136.3, 134.6, 132.8, 131.3, 129.4, 128.4, 127.5, 124.2, 124.0, 122.8, 121.0, 120.1, 117.8, 114.4, 112.5, 111.9, 110.6, 110.4, 21.9 (One carbon overlapped.)

HRMS (APCI): calcd for $C_{23}H_{18}NO_2$: *m/z* 340.1338 $[M + H]^+$, found 340.1327.

IR (KBr): 3503, 3408, 3060, 2923, 1621, 1496, 1442, 1171, 810, 751 cm^{-1}.

mp: 128-130 °C. White solid.

Enantiomeric excess: 84%, determined by HPLC (Chiralpak IA, hexane/2-popanol = 4/1; flow rate 1.0 mL/min; 25 °C; 230 nm) first peak: t_R = 19.2 min, second peak: t_R = 26.1 min. $[\alpha]_D^{20}$ –41.54 (*c* 0.72, $CHCl_3$) for 84% ee.

4-(2-hydroxy naphthalene-1-yl)-6-(4-hydroxyphenyl)-9*H*-carbazol-3-ol (20c)

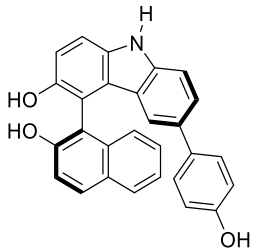

^{1}H NMR (400 MHz, $(CD_3)_2CO$): δ 10.19 (s, 1H), 8.20 (s, 1H), 8.02 (d, *J* = 9.2 Hz, 1H), 7.97 (d, *J* = 8.7 Hz, 1H), 7.85 (s, 1H), 7.53 (d, *J* = 8.7 Hz, 1H), 7.45-7.43 (m, 3H), 7.37-7.30 (m, 3H), 7.25-7.20 (m, 2H), 6.96-6.93 (m, 2H), 6.77-6.73 (m, 2H), 6.70 (s, 1H).

^{13}C NMR (100 MHz, $(CD_3)_2CO$): δ 156.4, 153.6, 149.5, 140.5, 135.7, 134.7, 133.9, 131.4, 130.1, 129.6, 128.4, 127.8, 126.6, 125.2, 124,2, 124.1, 123.8, 123.3, 119.8, 119.1, 116.0, 115.9, 115.8, 114.7, 111.8, 111.0.

HRMS (APCI): calcd for $C_{28}H_{20}NO_3$: *m/z* 418.1443 $[M + H]^+$, found 418.1439.

IR (KBr): 3408, 2925, 1704, 1469, 1269, 1237, 1269, 1172, 811 cm^{-1}.

mp: 165-167°C. White solid.

Enantiomeric excess: 83%, determined by HPLC (Chiralpak IC-3, hexane/2-popanol = 4/1; flow rate 1.0 mL/min; 25 °C; 230 nm) first peak: t_R = 10.5 min, second peak: t_R = 16.1 min. $[\alpha]_D^{23}$ –72.48 (*c* 0.63, EtOAc) for 83% ee.

11-(2-hydroxy naphthalene-1-yl)-7*H*-benzo[*c*]carbazol-10-ol (20g)

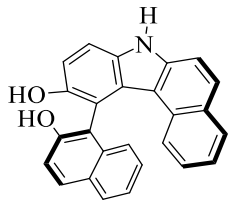

^{1}H NMR (400 MHz, $(CD_3)_2CO$): δ 10.87 (s, 1H), 8.11 (d, *J* = 9.2 Hz, 1H), 7.96 (d, *J* = 8.2 Hz, 1H), 7.87 (s, 1H), 7.78-7.70 (m, 4H), 7.44 (d, *J* = 8.7 Hz, 1H), 7.30 (d, *J* = 8.7 Hz, 2H), 7.25 (ddd, *J* = 8.4, 6.9, 1.4 Hz, 1H), 7.15 (ddd, *J* = 8.4 , 6.9, 0.9 Hz, 1H), 7.08 (s, 1H), 7.05 (ddd, *J* = 8.2, 6.9, 0.9 Hz, 1H), 6.76 (d, *J* = 8.7 Hz, 1 H), 6.60 (ddd, *J* = 8.7, 6.9, 1.8 Hz, 1H).

^{13}C NMR (100 MHz, $(CD_3)_2CO$): δ 154.3, 150.0, 139.4, 135.8, 134.8, 130.4, 129.6, 129.5, 128.9, 128.4, 128.0, 126.71, 125.66, 125.7, 125.6, 125.5, 123.4, 122.1, 119.14, 119.11, 116.6, 114.9, 113.8, 113.6, 112.8. (One carbon overlapped.)

HRMS (APCI): calcd for $C_{26}H_{18}NO_2$: *m/z* 376.1338 $[M + H]^+$, found 376.1334.

IR (KBr): 3510, 3491, 3400, 3062, 1619, 1389, 1344, 1195, 1151, 816, 753, 505 cm^{-1}.

mp: 268-270 °C. White solid.

Enantiomeric excess:73%, determined by HPLC (Chiralpak IA, hexane/2-popanol = 7/1; flow rate 1.0 mL/min; 25 °C; 230 nm) first peak: t_R = 40.4 min, second peak: t_R = 46.8 min.

$[\alpha]_D^{24}$ –9.48 (*c* 0.68, EtOAc) for 73% ee.

Chapter 4

4.1 Iron Catalyzed Asymmetric Hetro-coupling of 2-Naphthols with β-Ketoesters.

Metal-catalyzed cross-dehydrogenative coupling (CDC) or hetero coupling reactions have emerged as a powerful tool to synthesize new C-C bonds through the coupling of two CH bonds under oxidizing conditions. The development of this chemistry is particularly important as it offers a great probability to reduce the reliance of synthetic chemistry on classical cross-coupling reactions that rely heavily on the pre-functionalization of the coupling partners and noble metals.[39] This chapter will be exclusively focused on the iron-catalysed hetero-coupling of 2-naphthol with β-Ketoesters.

In 2017 Pappo research group has reported the cross dehydrogenative coupling of 2-naphthols with β-Ketoesters using chiral iron phosphate complex as shown in the (**Scheme 12**).[40]

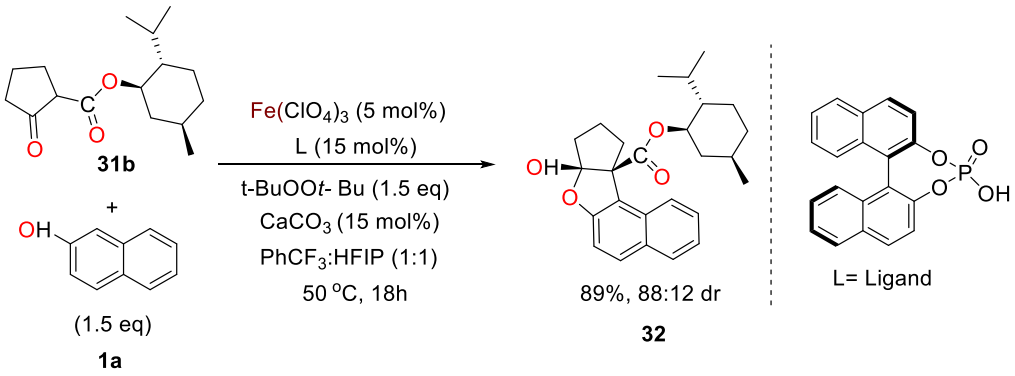

Scheme 12. Oxidative cross-coupling of 2-naphthol by chiral iron phosphate complex

The cross-coupling between 2-naphthol **1a** with chiral β-ketoester(-Menthyl) **31b** was performed using Iron complex under the standard oxidative reaction conditions to afford **32** in 89% yield with 88:12 dr and er. In this report, Pappo utilized chiral **31b,** where the diastereomeric ratio was mentioned for nonchiral compounds. The successful results on oxidative hetero-coupling using chiral vanadium complex inspired us to explore further applications for hetero coupling using 3-hydroxy carbazole **9a** and β-ketoester **31.**

4.2 Optimization of Reaction Condition:

Initially, the standard optimized hetero-coupling reaction conditions discussed in **Chapter 3** were applied as shown in (**Scheme. 13).** A *rac* product formation was obtained with 52% yield using previously optimized conditions (entry 1). Further maintaining the same solvent, a chiral vanadium catalyst (S_a,*S*)-**8b** was used (entry 2); which showed a *matched pair* with 3-

hydroxycarbazole **9p** and β-ketoester **31c**, resulting in 34 % yield and 28 % ee. Subsequently, the vanadium catalyst (S_a,*S*)-**8b** was tried with chlorobenzene as the solvent provided the product with 70 % yield and 82 % ee with a dr ratio of 10:1. The catalyst (R_a,*S*)-**30** in chlorobenzene as the solvent resulted into low yield with 84 % ee (entry 4). On the other hand, the utilization of the additive (LiCl) along with (S_a,*S*)-**8b** vanadium catalyst did not result in satisfactory results.

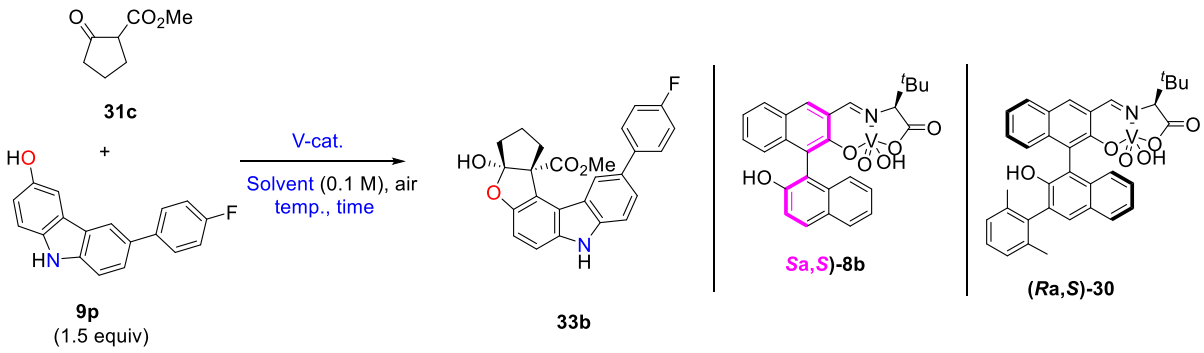

entry	solvents	temp.(°C)	V-cat.(10 mol%)	time.(h)	addtive	yield(%)[a]	ee	dr
1	1,4-Dioxane	30	(*Ra*,*S*)-**30**	96	LiCl	52	*rac*	-
2	1,4-Dioxane	50	(*Sa*,*S*)-**8b**	24	-	34	28	10:1
3	PhCl	30	(*Sa*,*S*)-**8b**	24	-	70	82	10:3
4	PhCl	50	(*Ra*,*S*)-**30**	24	-	48	84	-
5	PhCl	50	(*Sa*,*S*)-**8b**	24	LiCl	20	62	10:1
6	PhCl	50	(*Sa*,*S*)-**8b**	24	-	78	80	<20:1

[a]Isolated yields. [b] 3.0 equiv. used additive.

Scheme. 13 Optimization of reaction conditions

Finally, a slight increase in the temperature to 50 °C successfully delivered the product **33b** in 78% yield along with 80% ee and 20:1 dr as shown in entry 6.

4.3 Substrate Scope:

The optimized reaction conditions were explored for coupling of 3-hydroxycarbazoles **9** with β-ketoester **31c** using vanadium(V) catalyst as shown in (**Scheme 14**). A series of hydroxycarbazoles were converted into the cis-products **33a–d** and **33i** in moderate to good yields with up to 88% ee and >20: 1 dr. The hetero-coupling products **33e′** and **33f′** were obtained in the trans-form (>20: 1 dr) due to the steric hindrance generated by substituent at the 5-position of substrate **9**. Furthermore, the absolute configuration of **33i** was determined as (*R*, *S*) through X-ray crystallographic analysis.

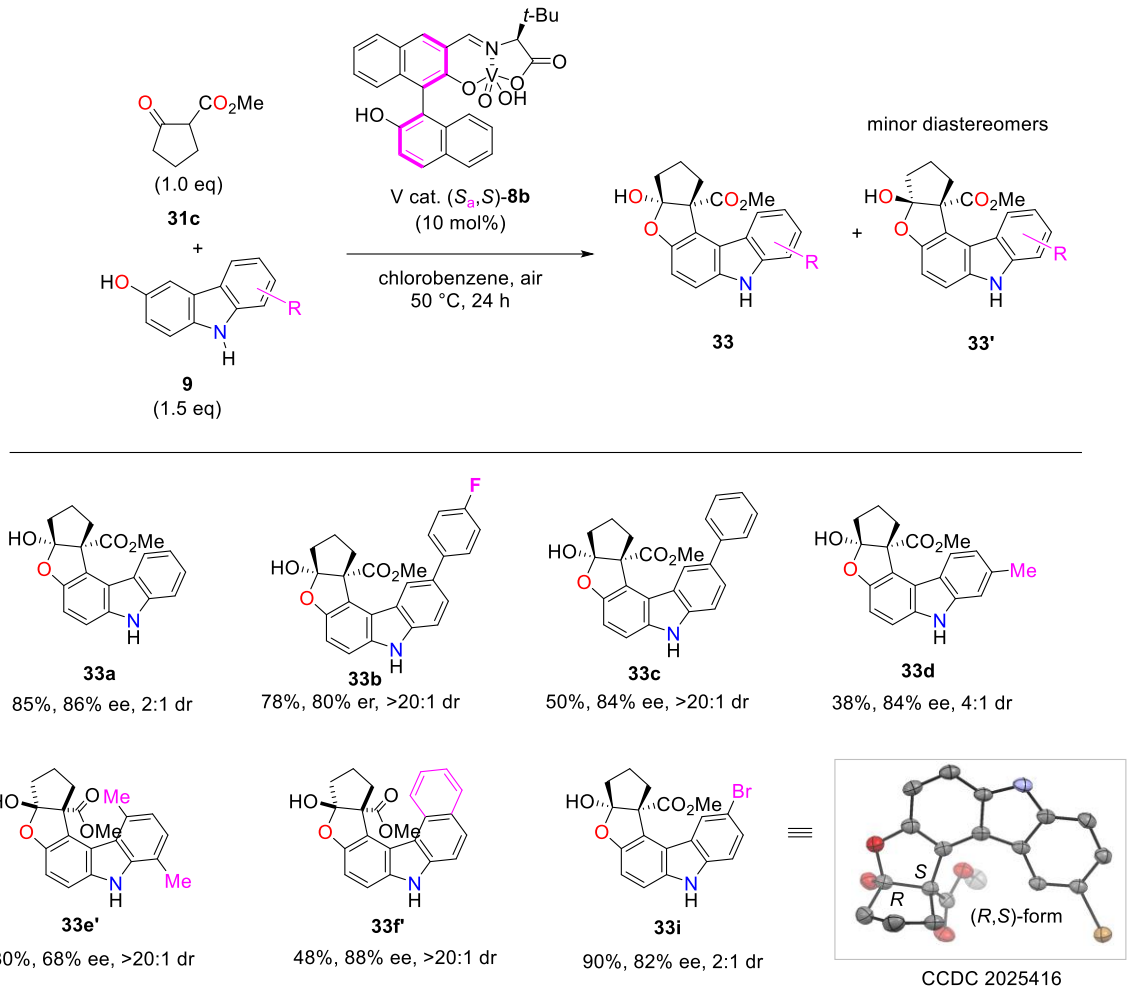

Scheme. 14 The substrate scope

4.4 Experimental section:

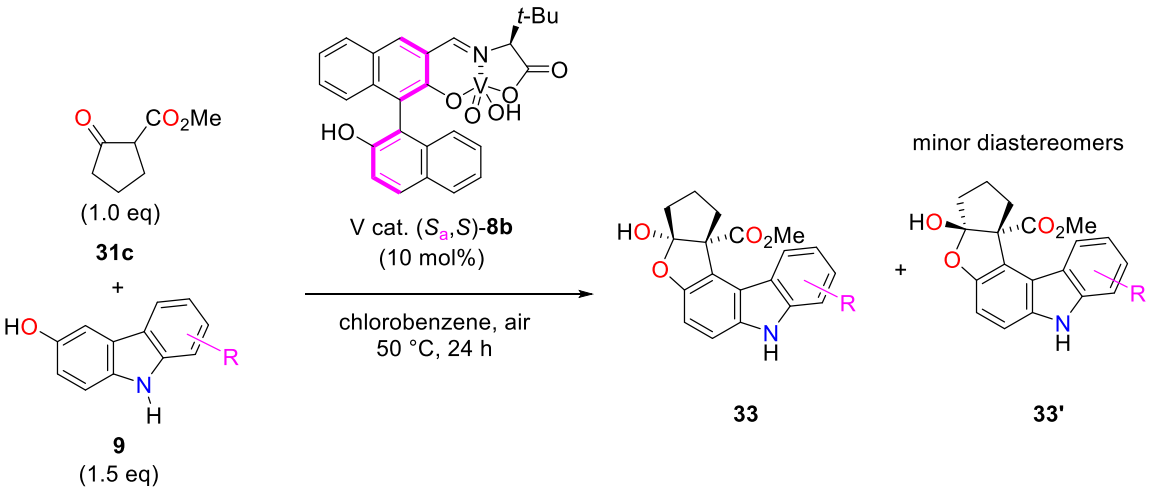

Scheme 15. Oxidative hetero coupling general reaction

General Procedures: -

To a stirred solution of 3-hydroxycarbazole **9** (0.52 mmol) and vanadium catalyst (S_a,*S*)-**8b** (10 mol %) was taken in a chem-station vial then methyl 2-oxocyclopentanecarboxylate **31c** (0.35 mmol) was dissolved in chlorobenzene (0.1 M) was added to the reaction mixture at the room temperature. The reaction mixture was stirred at 50 °C for 24 h., under the air atmosphere. After completion of the reaction mixture was passed through a silica bed. The dark green filtrate was collected and evaporated under reduced pressure. Purification was done by column chromatography in 20% ethyl acetate/ hexane as an eluent to afford a white solid.

Methyl 3a-hydroxy-1,2,3,3a-tetrahydrocyclopenta [4,5] furo[2,3-c] carbazole-11d(7H)-carboxylate (33a)

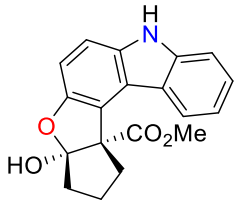

(**Major**)

^{1}H NMR (400 MHz, $CDCl_3$) δ 8.06 (s, 1H), 7.80 (d, *J* = 7.3 Hz, 1H), 7.43-7.38 (m, 2H), 7.26 (d, *J* = 1.8 Hz, 1H), 7.20-7.16 (m, 1H), 6.97 (d, *J* = 8.7 Hz, 1H), 3.94 (s, 1H), 3.70 (s, 3H), 3.08-3.03 (m, 1H), 2.44-2.34 (m, 2H), 2.17-2.10 (m, 1H), 1.90-1.84 (m, 1H), 1.60-1.54 (m, 1H)

(Minor)

^{1}H NMR (400 MHz, $CDCl_3$) δ 7.99-7.97 (m, 1H), 7.90 (s, 1H), 7.42 (s, 1H), 7.39-7.38 (m, 2H), 7.20-7.16 (m, 2H), 5.19 (s, 1H), 3.81 (s, 3H), 2.65-2.62 (m, 1H), 2.48-2.36 (m, 1H), 2.25-2.08 (m, 2H), 1.82-1.75 (m, 1H), 1.55-1.45 (m, 1H)

(**Major**)

^{13}C-NMR (101 MHz, $CDCl_3$) δ 172.7, 153.0, 140.6, 135.4, 126.1, 122.3, 121.3, 120.8, 120.7, 119.5, 119.3, 111.0, 110.9, 108.1, 65.2, 53.1, 39.8, 34.8, 22.8.

(Minor)

^{13}C-NMR (151 MHz, $CDCl_3$) δ 173.4, 152.7, 140.4, 134.9, 128.3, 126.1, 124.6, 123.2, 120.5, 119.9, 119.3, 110.7, 106.2, 99.8, 63.0, 53.0, 40.4, 37.6, 22.0.

HRMS (ESI): calcd for $C_{19}H_{17}NO_4$: *m/z* 323.12 $[M + Na]^+$, found 346.1046.

(Major)

IR (KBr): 3413, 2953, 1720, 1496, 1442, 1321, 1277, 1101, 937 cm^{-1}

(Minor)

IR (KBr): 3413, 2959, 1715, 1458, 1250, 1096, 860 cm^{-1}

mp: 98-102 ºC (White Solid) **(Major)**

196-200 ºC (White Solid) **(Minor)**

Enantiomeric ratio: dr 2:1

(Major) 86% ee, determined by HPLC (Chiral Pak IA, hexane/2-propanol = 7/1; flow rate 1.0 mL/min; 25 °C; 350 nm) first peak: t_R = 16.65 min, second peak: t_R = 19.3 min.

(Minor) 76% ee, determined by HPLC (Chiral Pak IA, hexane/2-propanol = 7/1; flow rate 1.0 mL/min; 25 °C; 360 nm) first peak: t_R = 28.48 min, second peak: t_R = 48.94 min.

$Major[\alpha]_D^{29}$ +5.3 (*c* 0.32, $CHCl_3$) for 86% ee. **(Major)**

$[\alpha]_D^{29}$ +25.62 (*c* 0.32, $CHCl_3$) for 76% ee. **(Minor)**

Methyl10-(4-fluorophenyl)-3a-hydroxy-1,2,3,3a-tetrahydrocyclopenta[4,5]furo[2,3-c]carbazole-11d(7H)-carboxylate (**33b)**

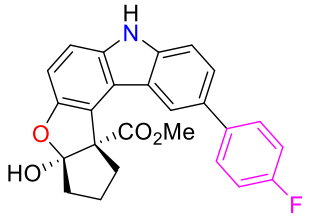

^{1}H NMR (400 MHz, $CDCl_3$) δ 8.08 (s, 1H), 8.02 (t, *J* = 0.9 Hz, 1H), 7.64-7.59 (m, 3H), 7.46 (d, *J* = 8.2 Hz, 1H), 7.29 (d, *J* = 8.7 Hz, 1H), 7.20-7.15 (m, 2H), 6.98 (d, *J* = 8.2 Hz, 1H), 4.01 (s, 1H), 3.71 (s, 3H), 3.13-3.06 (m, 1H), 2.45-2.38 (m, 2H), 2.16-2.10 (m, 1H), 1.90-1.84 (m, 1H), 1.60-1.54 (m, 1H)

^{13}C-NMR (101 MHz, $CDCl_3$**)** δ 172.7, 162.15 (d, J_{C-F} = 246.33 Hz), 153.1, 139.9, 137.9, 135.9, 131.8, 128.5, 128.4, 125.4, 121.9, 120.9, 120.6 (d, J_{C-F} = 30.67 Hz), 119.3, 115.82 (d, J_{C-F} = 22.04 Hz), 111.2, 111.1, 108.4, 65.2, 53.1, 39.8, 34.8, 31.7, 22.8, 14.2.

^{19}F NMR (565 MHz, $CDCl_3$): δ –120.02

HRMS (ESI): calcd for $C_{25}H_{20}FNO_4$: *m/z* 417.14 $[M + Na]^+$, found 440.126

IR (KBr): 3408, 2951, 1716, 1488, 1254, 1227, 1091, 944, 808 cm^{-1}

mp: 116-120 ºC (White Solid)

Enantiomeric ratio: dr < 20:1

80% ee, determined by HPLC (Chiral Pak IA, hexane/2-propanol = 7/1; flow rate 1.0 mL/min; 25 °C; 315 nm) first peak: t_R = 17.62 min, second peak: t_R = 26.71 min.

$[\alpha]_D^{28}$ -10.5 (*c* 0.40, $CHCl_3$) for 80% ee.

Methyl3a-hydroxy-10-phenyl-1,2,3,3a-tetrahydrocyclopenta[4,5]furo[2,3-c]carbazole-11d(7H)-carboxylate (33C)

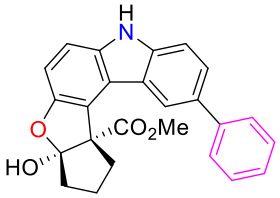

^{1}H NMR (400 MHz, $CDCl_3$) δ 8.08 (d, *J* = 1.8 Hz, 2H), 7.68 (dd, *J* = 8.2, 1.4 Hz, 3H), 7.51-7.43 (m, 3H), 7.36-7.32 (m, 1H), 7.25 (d, *J* = 1.4 Hz, 1H), 6.97 (d, *J* = 8.7 Hz, 1H), 4.07 (s, 1H), 3.72 (s, 3H), 3.13-3.05 (m, 1H), 2.44-2.38 (m, 2H), 2.21-2.13 (m, 1H), 1.89-1.83 (m, 1H), 1.60-1.51 (m, 1H)

^{13}C-NMR (101 MHz, $CDCl_3$) δ 172.7, 153.1, 141.8, 140.0, 135.9, 132.8, 129.0, 127.1, 126.6, 125.6, 121.9, 120.9, 120.8, 120.6, 119.4, 111.2, 111.1, 108.3, 65.2, 53.1, 39.8, 34.8, 22.8

HRMS (ESI): calcd for $C_{25}H_{21}NO_4$: *m/z* 399.15 $[M + Na]^+$, found 422.135

IR (KBr): 3409, 3376, 2943, 1704, 1600, 1491, 1260, 1118, 937, 756 cm^{-1}

mp: 118-124 ^{o}C (White Solid)

Enantiomeric ratio: dr < 20:1

84% ee, determined by HPLC (Chiral Pak IA, hexane/2-propanol = 7/1; flow rate 1.0 mL/min; 25 °C; 315 nm) first peak: t_R = 17.06 min, second peak: t_R = 23.23 min.

$[\alpha]_D^{28}$ +0.6 (*c* 0.39, $CHCl_3$) for 92:8 er.

Methyl 3a-hydroxy-9-methyl-1,2,3,3a-tetrahydrocyclopenta [4,5] furo[2,3-c] carbazole-11d(7H)-carboxylate (33d)

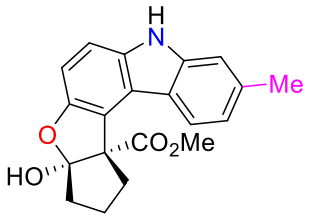

(Major)

^{1}H NMR (400 MHz, $CDCl_3$) δ 7.91 (s, 1H), 7.66 (d, *J* = 8.2 Hz, 1H), 7.23 (t, *J* = 8.9 Hz, 1H), 7.18 (s, 1H), 7.01-6.99 (m, 1H), 6.92 (d, *J* = 8.7 Hz, 1H), 3.94 (s, 1H), 3.69 (s, 3H), 3.07-3.02 (m, 1H), 2.50 (s, 3H), 2.42-2.32 (m, 2H), 2.18-2.16 (m, 1H), 1.89-1.82 (m, 1H), 1.59-1.53 (m, 1H)

(Minor)

^{1}H NMR (400 MHz, $CDCl_3$) δ 7.85 (d, J = 8.2 Hz, 1H), 7.78 (s, 1H), 7.37 (s, 1H), 7.15 (d, J = 16.0 Hz, 2H), 7.01 (d, J = 7.8 Hz, 1H), 5.20 (s, 1H), 3.81 (s, 3H), 2.64 (td, J = 12.5, 6.6 Hz, 1H), 2.50 (s, 3H), 2.43-2.37 (m, 1H), 2.25-2.20 (m, 1H), 2.18-2.10 (m, 1H), 1.80-1.77 (m, 1H), 1.58-1.49 (m, 1H)

(Major)

^{13}C-NMR (101 MHz, $CDCl_3$**)** δ 172.8, 153.0, 141.1, 136.5, 135.4, 122.0, 121.1, 120.7, 120.4, 119.4, 119.0, 110.9, 110.8, 107.4, 65.1, 53.1, 39.7, 34.8, 22.8, 22.1.

(Minor)

^{13}C-NMR (151 MHz, $CDCl_3$**)** δ 173.5, 152.7, 140.9, 136.3, 134.9, 127.5, 124.7, 121.0, 120.9, 120.1, 119.9, 110.8, 106.0, 99.6, 62.9, 53.0, 40.4, 37.6, 22.2, 22.0

HRMS (ESI): calcd for $C_{20}H_{19}NO_4$: *m/z* 337.13 $[M + Na]^+$, found 360.120

(Major)

IR (KBr): 3485, 3392, 2948, 1726, 1616, 1436, 1260, 1123, 937, 805 cm^{-1}

(Minor)

IR (KBr): 3402, 2945, 1711, 1444, 1254, 1091, 792 cm^{-1}

mp: 215-219 ^{o}C (White Solid) **(Major)**

178-182 ^{o}C (White Solid) **(Minor)**

Enantiomeric ratio: dr 4:1

(Major) 84% ee, determined by HPLC (Chiral Pak IA, hexane/2-propanol = 7/1; flow rate 1.0 mL/min; 25 °C; 315 nm) first peak: t_R = 18.46 min, second peak: t_R = 23.60 min.

(Minor) 90:10 er, determined by HPLC (Chiral Pak IA, hexane/2-propanol = 7/1; flow rate 1.0 mL/min; 25 °C; 300 nm) first peak: t_R = 34.28 min, second peak: t_R = 55.58 min.

$[\alpha]_D^{29}$ +26.66 (*c* 0.33, $CHCl_3$) for 84% ee. **(Major)**

$[\alpha]_D^{29}$ +59.39 (*c* 0.32, $CHCl_3$) for 80 ee. **(Minor)**

Methyl3a-hydroxy-1,2,3,3a-tetrahydrobenzo[c]cyclopenta[4,5]furo[3,2-g]carbazole-13e(7H)-carboxylate (33f')

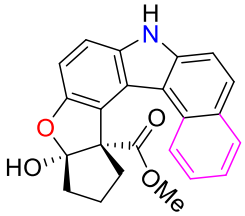

^{1}H NMR (400 MHz, $CDCl_3$) δ 8.62 (d, J = 8.2 Hz, 1H), 8.29 (s, 1H), 7.97 (d, J = 8.2 Hz, 1H), 7.91 (s, 1H), 7.82 (d, J = 8.7 Hz, 1H), 7.68 (td, J = 7.7, 1.2 Hz, 1H), 7.58-7.55 (m, 1H), 7.48-

7.44 (m, 1H), 7.29 (d, *J* = 4.1 Hz, 1H), 5.22 (s, 1H), 3.84 (s, 3H), 2.69-2.60 (m, 1H), 2.48-2.43 (m, 1H), 2.29-2.24 (m, 1H), 2.19-2.12 (m, 1H), 1.84-1.78 (m, 1H), 1.55-1.49 (m, 1H)

^{13}C-NMR (151 MHz, $CDCl_3$**)** δ 173.5, 153.4, 138.1, 134.0, 129.9, 129.3, 129.1, 127.7, 127.1, 127.0, 124.9, 123.1, 123.0, 120.0, 115.3, 112.7, 106.6, 101.3, 63.0, 53.0, 40.4, 37.7, 22.1

HRMS (ESI): calcd for $C_{23}H_{19}NO_4$: *m/z* 373.13 $[M + Na]^+$, found 396.120

IR (KBr): 3403, 2953, 1720, 1463, 1254, 1085, 937, 800 cm^{-1}

mp: 146-150 ºC (White Solid)

Enantiomeric ratio: dr < 20:1

88% ee, determined by HPLC (Chiral Pak IA, hexane/2-propanol = 7/1; flow rate 1.0 mL/min; 25 °C; 315 nm) first peak: t_R = 17.41 min, second peak: t_R = 29.60 min.

$[\alpha]_D^{28}$ +38.57 (*c* 0.35, $CHCl_3$) for 88% ee.

Methyl10-bromo-3a-hydroxy-1,2,3,3a-tetrahydrocyclopenta[4,5]furo[2,3-c]carbazole-11d(7H)-carboxylate (33i)

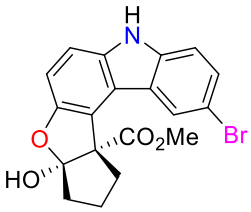

(**Major**)

^{1}H NMR (400 MHz, $CDCl_3$) δ 8.11 (s, 1H), 7.94 (d, *J* = 1.8 Hz, 1H), 7.47 (dd, *J* = 8.2, 1.8 Hz, 1H), 7.28 (d, *J* = 6.0 Hz, 1H), 7.25 (s, 1H), 6.98 (d, *J* = 8.7 Hz, 1H), 4.17 (s, 1H), 3.78 (s, 3H), 3.08-3.00 (m, 1H), 2.42-2.33 (m, 2H), 2.20-2.11 (m, 1H), 1.89-1.70 (m, 1H), 1.61-1.49 (m, 1H)

(**Minor**)

^{1}H NMR (400 MHz, $CDCl_3$) δ 8.08 (d, *J* = 2.3 Hz, 1H), 7.94 (s, 1H), 7.45 (dd, *J* = 8.7, 1.8 Hz, 1H), 7.35 (s, 1H), 7.25 (d, *J* = 6.9 Hz, 1H), 7.17 (d, *J* = 0.9 Hz, 1H), 5.15 (s, 1H), 3.81 (s, 3H), 2.69-2.63 (m, 1H), 2.50-2.38 (m, 1H), 2.24-2.08 (m, 2H), 1.83-1.76 (m, 1H), 1.56-1.48 (m, 1H)

(**Major**)

^{13}C-NMR (101 MHz, $CDCl_3$) δ 172.8, 153.2, 139.1, 135.8, 128.8, 124.8, 122.9, 120.8, 118.2, 112.3, 112.0, 111.4, 109.0, 65.0, 53.1, 39.8, 34.8, 22.8

(**Minor**)

^{13}C-NMR (151 MHz, $CDCl_3$) δ 173.3, 152.9, 138.9, 135.3, 129.3, 128.7, 125.0, 123.5, 123.1, 120.1, 112.2, 112.0, 106.5, 99.9, 63, 53.1, 40.3, 37.7, 22.1

HRMS (ESI): calcd for $C_{19}H_{16}BrNO_4$: *m/z* 401.03 $[M + Na]^+$, found 424.015

(Major)

IR (KBr): 3408, 2951, 1721, 1493, 1439, 1281, 1096, 944, 797 cm^{-1}

(Minor)

IR (KBr): 3418, 2951, 1721, 1466, 1270, 1096, 949, 868, 802, 753 cm^{-1}

mp: 105-110 ^oC (White Solid) **(Major)**

220-225 ^oC (White Solid) **(Minor)**

Enantiomeric ratio: dr 2:1

(Major) 82% ee, determined by HPLC (Chiral Pak IA, hexane/2-propanol = 7/1; flow rate 1.0 mL/min; 25 °C; 309 nm) first peak: t_R = 14.96 min, second peak: t_R = 20.07 min.

(Minor) 80% ee, determined by HPLC (Chiral Pak IA, hexane/2-propanol = 7/1; flow rate 1.0 mL/min; 25 °C; 315 nm) first peak: t_R = 23.80 min, second peak: t_R = 53.98 min.

$[\alpha]_D^{28}$ -2.25 (*c* 0.40, $CHCl_3$) for 82% ee. **(Major)**

$[\alpha]_D^{28}$ +39.5 (*c* 0.40, $CHCl_3$) for 80% ee. **(Minor)**

4.5 References:

39. (a) Girard, S. A.; Knauber, T.; Li, C. J. *Angew. Chem., Int. Ed.* **2014**, *53*, 74. (b) Liu, C.; Zhang, H.; Shi, W.; Lei, A. *Chem. Rev.* **2011**, *111*, 1780. (c) Wu, Y.; Wang, J.; Mao, F.; Kwong, F. Y. *Chem. - Asian J.* **2014**, *9*, 26. (d) Yeung, C. S.; Dong, V. M. *Chem. Rev.* **2011**, *111*, 1215. (e) Scheuermann, C. *J. Chem. - Asian J.* **2010**, *5*, 436. (f) Li, C.-J. *Acc. Chem. Res.* **2009**, *42*, 335. (g) Li, Z.; Bohle, D. S.; Li, C.-*J. Proc. Natl. Acad. Sci. U. S. A.* **2006**, *103*, 8928.

40. Narute S.; Pappo D. *Org. Lett.* **2017**, *19*, 2917-2920.

5. Outlook of Ongoing Work

The recent advances in the chiral synthesis of biaryl moieties enabled the exploration of electron-rich ligands for metal-catalysed coupling reactions. Despite many methodologies that have been developed for chiral access to these compounds, new methods are widening the scope for further exploration. Especially, the oxidative hetero coupling reactions of hydroxyl naphthol and their derivatives are of great interest. However, the utilization of nitrogen-based compounds such as 2-naphthlymine is challenging due to reactivity and oxidation potential differences. Thus, it creates an opportunity for the exploration of hetero-coupled 2-naphthyl amine derivatives, which is currently underway in our laboratory.

5.1 Introduction:

Reported oxidative coupling methods for preparing optically pure NOBINs

Biaryls with axial chirality, such as 1,1'-bi-2-naphthols (BINOLs) and 2-amino-2'-hydroxy-1,1'-binaphthyl (NOBINs), serve as building blocks, ligands, and catalysts in asymmetric transformations.[41] Over the past three decades, many research groups have significantly contributed to the synthesis of axially chiral BINOLs, using vanadium, copper, iron, and ruthenium catalysis. Synthesis of axially chiral NOBINs molecules using oxidative direct coupling still has many challenges such as control of chemoselectivity, high enantioselectivity, and thorough mechanistic understanding.

In this context, recently, Tian and Tu reported[42] the first successful oxidative cross-coupling reaction based on the Cu(I)/SPDO (SPDO = spirocyclic pyrrolidine oxazoline) catalyst, which provides an access to enantioenriched 3,3'-disubstituted NOBINs up to 80% yield 96 % ee as shown in the (**Scheme 16A**).

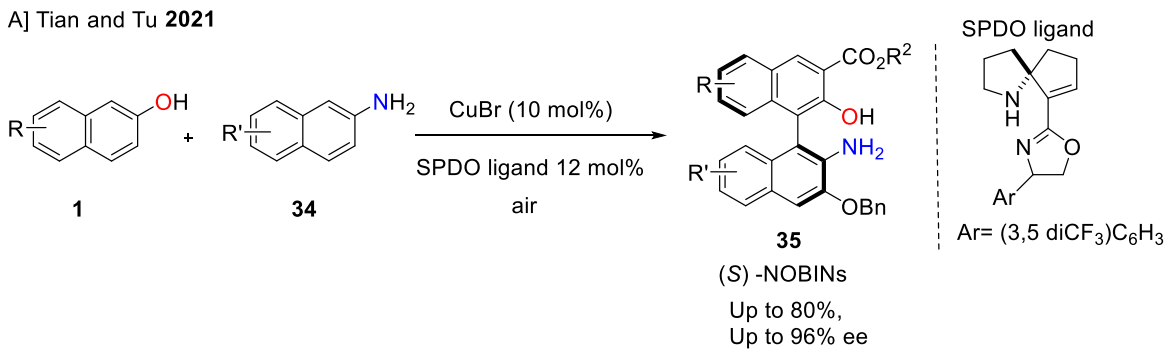

Scheme 16A. The reported oxidative coupling of NOBINs

Subsequently, Pappo has reported enantioselective oxidative coupling of **1** with **34** to give NOBINs using chiral iron disulfonate catalyst and strong oxidant as lauroyl peroxide.[8p] as shown in (**Scheme 16B)**. This strategy was based on the multi-coordinate Fe(III) complex (**Figure 4)** due to the multi-coordination of the site on the iron catalyst needing to be designed by using appropriate substrates.

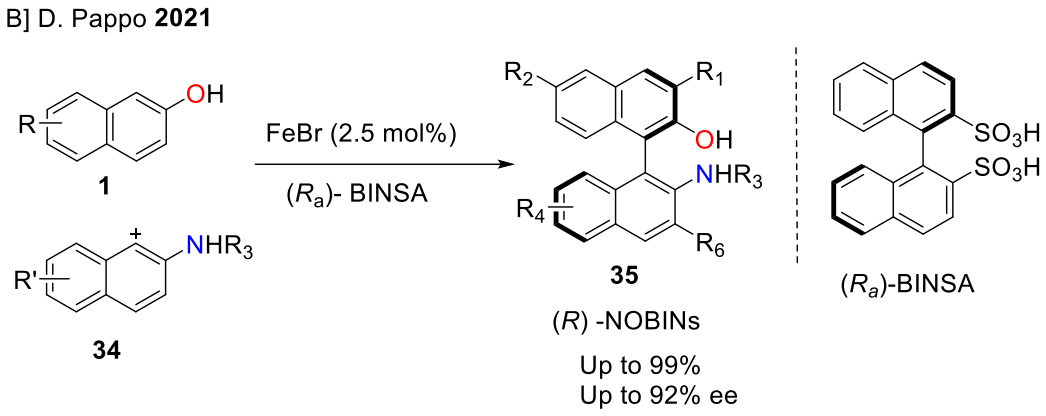

Scheme 16B. Chiral iron disulfonate catalyst for the enantioselective synthesis of NOBINs.

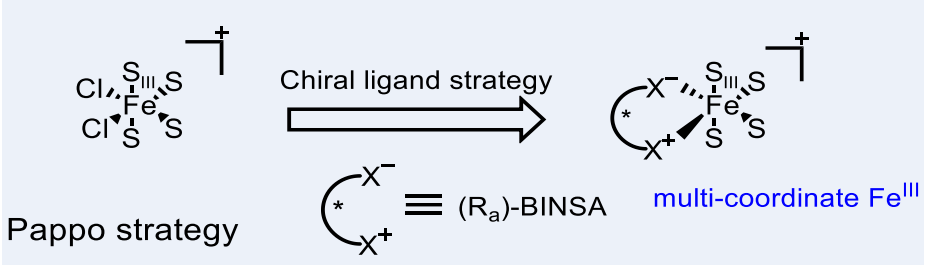

Figure 4 Multi coordinate Fe (III) Complex

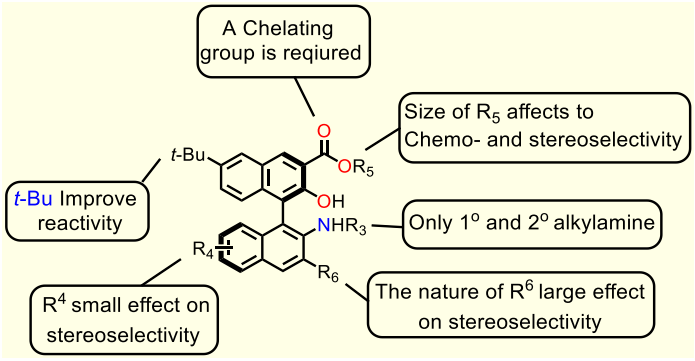

Figure 5 Limitations of substrate

Considering the high value of chiral NOBINs scaffolds in organic chemistry, there is an emerging need for their preparation by efficient, general, and direct scalable methods. Thus, we are currently exploring green chiral vanadium catalysts to develop hereto coupling reactions.

5.2 Ongoing Work:

Chiral vanadium(V) complex-catalyzed hetero coupling of *β*-naphthylamines *via* photoactivation

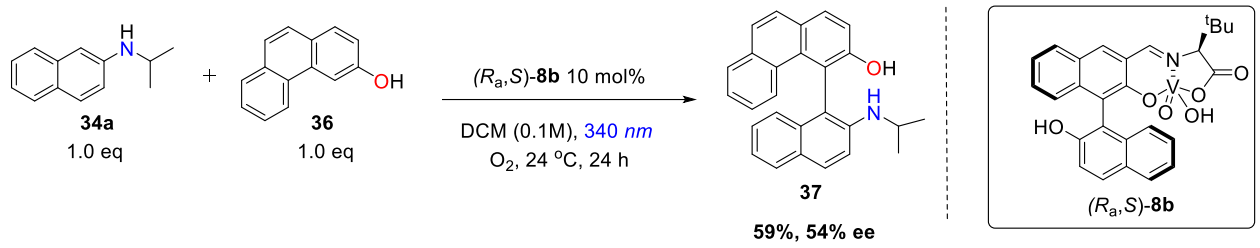

Scheme 17. Oxidative coupling of 2- naphthylamine *via* photoactivation.

Another interesting insight into the hetero-coupling reaction between *N-iso*-propyl-2-naphthylamine (**34a**) and 3-phenanthrol (**36**) using mono nuclear vanadium catalyst (R_a,*S*)-**8b** *via* photoactivation is shown in (**Scheme 17)**. In this reaction, the *N*-Isopropyl-2-naphthylamine was activated by using 340 *nm* LED light to provide **37** with moderate yield and enantioselectivity (59%, 54% ee) without any formation of byproducts. The hypothesized reaction mechanism *via* single electron transfer with radical-radical coupling is shown in **Scheme 18**. Further optimization is under progress through cooperative research with Ms Fan Duona in our research laboratory.

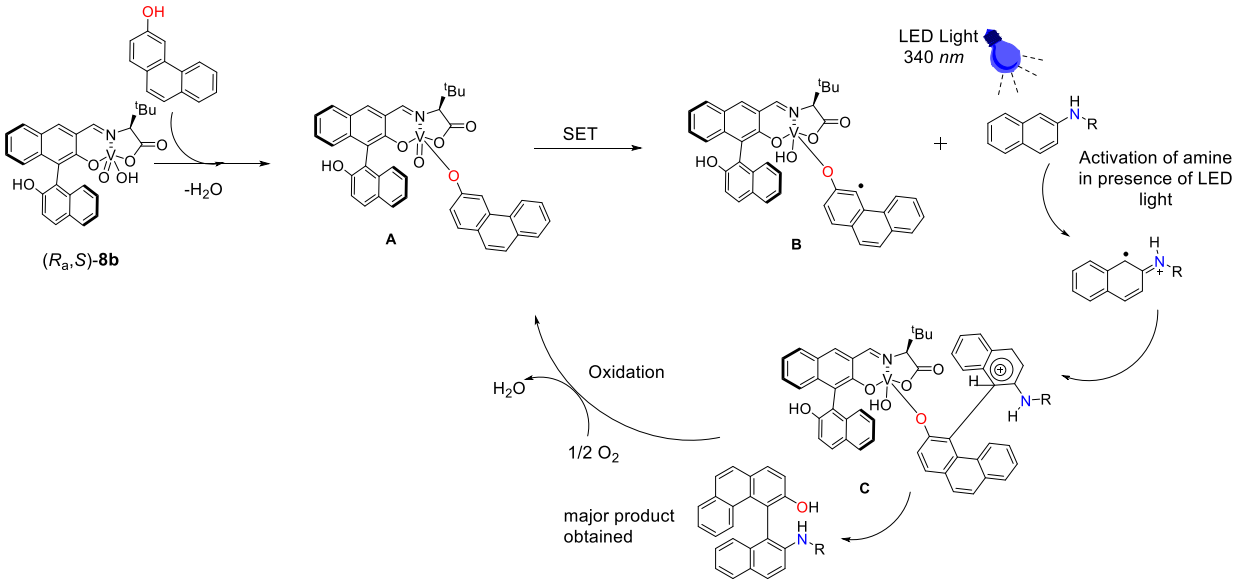

Scheme 18. Proposed hypothesis mechanism

5.3 References:

41. (a) Ding, K.; Li, X.; Ji, B.; Guo, H.; Kitamura, M. *Curr. Org. Synth.* **2005**, *2*, 499. (b) Liu, C.-X.; Zhang, W.-W.; Yin, S.-Y.; Gu, Q.; You, S.-L. *J. Am. Chem. Soc.* **2021**, *143*,14025.
42. Zhao, X.-J.; Li, Z.-H.; Ding, T.-M.; Tian, J.-M.; Tu, Y.-Q.; Wang, A.-F.; Xie, Y.-Y. *Angew. Chem., Int. Ed.* **2021**, *60*, 7061.

5.4 Conclusion:

A highly enantioselective oxidative coupling of 4-hydroxycarbazoles to form axially chiral dimeric hydroxycarbazoles was described in **Chapter 1**. The chiral vanadium(V) dinuclear complex (*R*a,*S*,*S*)-**10a** has proven to have high catalytic activity by activating hydroxycarbazole derivatives on both sides. Moreover, the DFT calculations have confirmed the axial chiral stability as well as the reactivity for 4-hydroxycarbazoles as shown in (**Scheme 19)**.

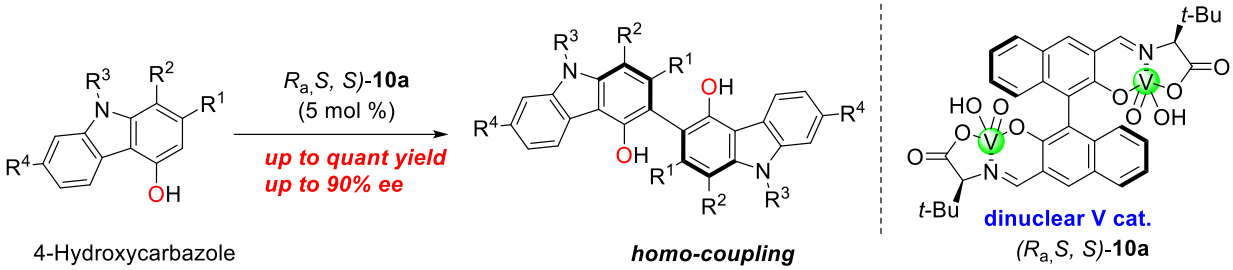

Scheme 19. First enantioselective homo-coupling of 4-hydroxycarbazole

A highly enantioselective and catalytic oxidative hetero-coupling of 3-hydroxycarbazoles **9** with 2-naphthols **1** using newly developed mononuclear vanadium(V) complex (*R*a,*S*)-**30** as shown in the **Scheme 20** was described in **Chapter 2**.

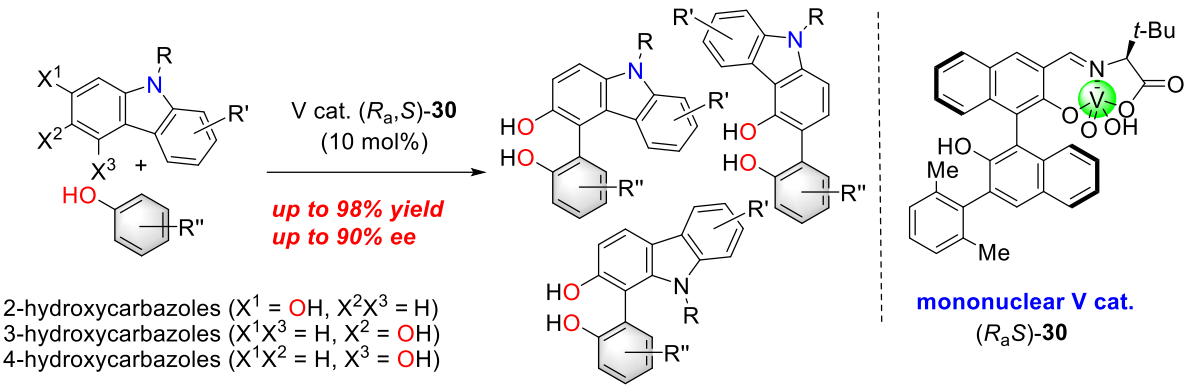

Scheme 20. First enantioselective hetero-coupling of hydroxycarbazole

This catalytic system successfully produced hetero-coupling products **20** with up to 98% yield and 90% ee by using two starting materials in a 1: 1 molar ratio, which is described in **Chapter 3**. Further exploration with 4- and 3-hydroxycarbazoles and β-ketoester **31c** substrates was also found to be appropriate for the chiral vanadium(V) catalysed oxidative hetero-couplings as described in **Chapter 4**. Additional mechanistic studies and development on hetero-coupling products *via* photoactivation and their potential applications as chiral catalysts are currently in progress as described in **Chapter 5**.

Acknowledgement

This thesis is the end of my journey in obtaining my Ph.D. completion of this doctoral dissertation was possible with the support of several people. First of all, I would like to express my deep gratitude, respect, and sincere appreciation to my research adviser **Prof. Hiroaki Sasai** and **Prof. Takayoshi Suzuki** for giving me a great opportunity to join a Ph.D. student in his research group. I am genuinely thankful for his constant support, suggestions, and encouragement. His financial support was very helpful during the hard time that makes me comfortable focusing on my research.

I pay special respect to Assoc. Prof. Shinobu Takizawa, for his continuous guidance, encouragement, and stimulating discussions throughout this research work. All the results reported in this thesis would not have been achieved without his constant guidance. Under his guidance, I successfully overcome many difficulties and learned a lot. Despite his busy time, he used to review my thesis progress gave his valuable suggestions and corrected them. Also, I would like to thank him for making me comfortable in the laboratory.

I would also like to thank all committee members for my doctoral defence, Prof. Takashi Kubo Prof. Michio Murata, and Assoc. Prof. Takeyuki Suzuki. I would like to thank Asst. Prof. Makoto Sako, Asst. Prof. Masaru Kondo and Asst. Prof. Tsukasa Abe for their helpful suggestions, directions, and encouragement.

I am deeply appreciating the help received from the technical staff of the Comprehensive Analysis Center (CAC) at Osaka University, Mr Tsunayoshi Takehara for X-ray crystallographic analysis, Mr Hitoshi Haneoka and Dr Da-Yang Zhou for NMR measurements, and Mr Tsuyoshi Matsuzaki for HRMS measurements.

I would like to express deep gratitude to everyone at the Institute of Scientific and Industrial Research, Osaka University, and the Department of Synthetic Organic Chemistry Laboratory for their help in experiments and everyday life, and for having a pleasant research life. Dr Kumar Ankit, Dr H.D.P. Wathsala, Dr Khalid Md Imrul and Dr Akimasa Sugizaki. Also, I would like to thank my lab mates Ms Tin Zar Aye, Mr Chandu G. Krishan, Mr Mohamed Salem, Ms Fan Duona, Ms Meghana Sasi, and Mr Ahmed Sabri. I am thankful to

the previous member of our laboratory Mr Keigo Higashida and Mr Hanseok Park for their help.

I would like to thank Ms Ayaka Honda and Ms Kaya Yoshino for taking care of us in our daily office work and miscellaneous tasks.

I would like to thank Dr Sandip Pujari (my research supervisor in PI industries, India), Dr Yogesh Dhage and Dr Sachin Narute, Dr Prashant Pavashe, and Dr Sharayu Kasar (QST, Chiba, Japan) for their motivation and recommendation to fulfil my dream of getting Ph.D. degree.

Furthermore, I would like to express my deep gratitude to the Japan Student Services Organization. (Honors Scholarship) and Japan Educational Exchanges and Services (JEES Sponsor-Crowned Scholarship) providing financial assistance to pursue my graduation comfortably. Finally, I would like to express my deep gratitude to my friends and acquaintances who supported me in various ways, and to my family who kindly supported my long student life.

Ganesh Tatya Kamble
Osaka University, Japan
August 2022